

การสังเคราะห์และศึกษาคุณสมบัติของซีควนเซียลอินเตอเพนเทอร์ทิงพอลิเมอร์เน็ตเวิร์คของ
พอลิยูรีเทนอะคริเลตและพอลิเบนซอกซาซีน

นายภยภัท พุดหอม

วิทยานิพนธ์นี้เป็นส่วนหนึ่งของการศึกษาตามหลักสูตรปริญญาวิทยาศาสตรมหาบัณฑิต
สาขาวิชาวิศวกรรมเคมี ภาควิชาวิศวกรรมเคมี
คณะวิศวกรรมศาสตร์ จุฬาลงกรณ์มหาวิทยาลัย

บทคัดย่อและแฟ้มข้อมูลฉบับเต็มของวิทยานิพนธ์ตั้งแต่ปีการศึกษา 2555-54 ที่ให้บริการในคลังปัญญาจุฬาฯ (CUIR)
เป็นแฟ้มข้อมูลของลิขสิทธิ์ของจุฬาลงกรณ์มหาวิทยาลัย

The abstract and full text of theses from the academic year 2011 in Chulalongkorn University Intellectual Repository (CUIR)
are the thesis authors' files submitted through the Graduate School.

SYNTHESIS AND CHARACTERIZATION OF SEQUENTIAL
INTERPENETRATING POLYMER NETWORKS OF POLYURETHANE
ACRYLATE AND POLYBENZOXAZINE

Mr. Kasiphat Pudhom

A Thesis Submitted in Partial Fulfillment of the Requirements
for the Degree of Master of Engineering Program in Chemical Engineering

Department of Chemical Engineering

Faculty of Engineering

Chulalongkorn University

Academic Year 2012

Copyright of Chulalongkorn University

Thesis Title SYNTHESIS AND CHARACTERIZATION OF SEQUENTIAL
INTERPENETRATING POLYMER NETWORKS OF
POLYURETHANE ACRYLATE AND POLYBENZOXAZINE

By Mr. Kasiphat Pudhom

Field of Study Chemical Engineering

Thesis Advisor Associate Professor Sarawut Rimdusit, Ph.D.

Thesis Co-advisor Associate Professor Neeracha Sanchavanakit, Ph.D.

Accepted by the Faculty of Engineering, Chulalongkorn University in
Partial Fulfillment of the Requirements for the Master's Degree

.....Dean of the Faculty of Engineering
(Associate Professor Boonsom Lerdhirunwong, Dr.Ing.)

THESIS COMMITTEE

..... Chairman
(Associate Professor Muenduen Phisalaphong, Ph.D.)

.....Thesis Advisor
(Associate Professor Sarawut Rimdusit, Ph.D.)

..... Thesis Co-advisor
(Associate Professor Neeracha Sanchavanakit, Ph.D.)

..... Examiner
(Associate Professor Seeroong Prichanont, Ph.D.)

..... External Examiner
(Phiriyatorn Suwanmala, Ph.D.)

กษิภัท พุดหอม: การสังเคราะห์และศึกษาคุณสมบัติของซีควนเชียลอินเตอร์เพเนทรทิงพอลิเมอร์เน็ตเวิร์คของพอลิยูรีเทนอะคริเลต-พอลิเบนซอกซาซีน (SYNTHESIS AND CHARACTERIZATION OF SEQUENTIAL INTERPENETRATING POLYMER NETWORKS OF POLYURETHANE ACRYLATE AND POLYBENZOXAZINE) อ. ที่ปริภษาวิทยานิพนธ์หลัก: รศ.ดร.ศราวุธ ริมคูลิต,
 อ. ที่ปริภษาวิทยานิพนธ์ร่วม: รศ.ดร.นिरชา สารชวณะภิจ, 87 หน้า.

งานวิจัยนี้มีจุดมุ่งหมายเพื่อพัฒนา สมบัติของสารเคลือบพอลิยูรีเทนอะคริเลตที่สามารถบ่มด้วยแสงอัลตราไวโอเลตผ่านการทำอัลลอยกับพอลิเบนซอกซาซีนที่สามารถบ่มด้วยความร้อนโดยพอลิเมอร์โครงข่ายลูกผสมของพอลิยูรีเทนอะคริเลตและพอลิเบนซอกซาซีนเตรียมได้จากการบ่มแบบซีควนเชียลโดยใช้แสงอัลตราไวโอเลตตามด้วยการบ่มด้วยความร้อน จากนั้นทำการศึกษาผลของการบ่มข้างต้นที่มีต่อสมบัติเชิงกลเชิงความร้อน และสมบัติทางกายของพอลิเมอร์อัลลอย ที่ได้จากการทดลองพบว่าพอลิเบนซอกซาซีนส่งผลกระทบต่อสมบัติของพอลิยูรีเทนอะคริเลต-พอลิเบนซอกซาซีนอัลลอย ทั้งนี้ฟิล์มพอลิเมอร์อัลลอยจากเรซินทั้งสองที่ผ่านการบ่มอย่างสมบูรณ์มีลักษณะ โปร่งใสและแสดงอุณหภูมิเปลี่ยนสถานะคล้ายแก้วเพียงค่าเดียว แสดงให้เห็นถึงลักษณะที่เข้ากันได้ดีหรืออีกนัยหนึ่งคือไม่เกิดการแยกเฟสระหว่างพอลิยูรีเทนอะคริเลตและพอลิเบนซอกซาซีน โมดูลัสสะสมที่สภาวะคล้ายแก้วและอุณหภูมิเปลี่ยนสถานะคล้ายแก้วของพอลิยูรีเทนอะคริเลตและพอลิเบนซอกซาซีนอัลลอยที่ได้จากการบ่มแบบซีควนเชียล มีค่าเพิ่มขึ้นตามการเพิ่มขึ้นของปริมาณเบนซอกซาซีน นอกจากนี้อุณหภูมิการสลายตัวทางความร้อนที่น้ำหนักของฟิล์มตัวอย่างลดลง 10 เปอร์เซ็นต์ พบว่ามีค่าค่อนข้างสูง ในขณะที่ปริมาณแก้วที่อุณหภูมิ 800 องศาเซลเซียส มีค่าเพิ่มสูงขึ้นตามปริมาณของพอลิเบนซอกซาซีนในพอลิเมอร์อัลลอยนอกจากนี้ ความแข็งของพื้นผิวและค่ามุมสัมผัสของน้ำของอัลลอยที่ได้ มีค่าเพิ่มสูงขึ้น ในขณะที่ค่าการดูดซึมน้ำและค่าการซึมผ่านของน้ำของฟิล์มลูกผสมมีแนวโน้มลดลงเมื่อเติมพอลิเบนซอกซาซีนลงไป ในพอลิเมอร์อัลลอย ดังนั้นการเพิ่มคุณสมบัติทางความร้อน ทางกล และทางกายภาพของโครงข่ายพอลิยูรีเทนอะคริเลตที่สามารถบ่มได้ด้วยแสงอัลตราไวโอเลตสามารถทำได้โดยการทำพอลิเมอร์โครงข่ายลูกผสมกับพอลิเบนซอกซาซีน ซึ่งจากการทดลองที่ได้พบว่า พอลิเมอร์อัลลอยจากพอลิยูรีเทนอะคริเลตกับพอลิเบนซอกซาซีนที่สัดส่วนการผสมที่ 50 /50โดยน้ำหนัก เป็นอัตราส่วนที่เหมาะสมที่สุดในการนำไปประยุกต์ใช้เป็นสารเคลือบผิวคุณภาพสูง

ภาควิชา.....วิศวกรรมเคมี..... ลายมือชื่อนิสิต.....
 สาขาวิชา.....วิศวกรรมเคมี..... ลายมือชื่อ อ.ที่ปริภษาวิทยานิพนธ์หลัก.....
 ปีการศึกษา..... 2555..... ลายมือชื่อ อ.ที่ปริภษาวิทยานิพนธ์ร่วม.....

5170606321 : MAJOR CHEMICAL ENGINEERING

KEYWORDS : POLYBENZOXAZINE/ URETHANE ACRYLATE / IPNs/ UV CURABLE

KASIPHAT PUDHOM: SYNTHESIS AND CHARACTERIZATION OF SEQUENTIAL INTERPENETRATING POLYMER NETWORKS OF POLYURETHANE ACRYLATE AND POLYBENZOXAZINE. ADVISOR: ASSOC. PROF. SARAWUT RIMDUSIT, Ph.D., CO-ADVISOR: ASSOC. PROF. NEERACHA SANCHAVANAKIT, Ph.D., 87 pp.

The purpose of this research is to improve performance of UV curable polyurethane acrylate coating by alloying with thermally curable polybenzoxazine. The hybrid polymer networks of polyurethane acrylate and polybenzoxazine were prepared by sequential cure methods i.e. UV cure method followed by thermal cure method. The effects of sequential cure methods were investigated in term of mechanical, thermal and physical properties of the resulting polymer alloy films. The experimental results revealed that the presence of the polybenzoxazine in the alloy network significantly affected the obtained properties of the PUA/BA-a alloys. The fully cured PUA/BA-a alloy films were transparent and showed only single glass transition temperature, suggesting high compatibility or no phase separation between the PUA and BA-a networks. The storage modulus in a glassy state and the glass transition temperatures (T_g) of PUA/BA-a alloys from the sequential cure method were found to substantially increase with increasing the BA-a mass fraction. Furthermore, T_d at 10% weight loss of the PUA/BA-a alloy films was relatively high whereas the char yield at 800°C was found to increase with an incorporation of the BA-a. Hardness, and water contact angle were enhanced whereas water absorption and water permeability of the alloy films were suppressed by the incorporation of the BA-a into the polymer alloys. As a consequence, thermal, mechanical and physical properties of the UV curable polyurethane acrylate networks can be positively tailored and enhanced by forming hybrid network with the BA-a. From the above results, the PUA/BA-a alloy at a 50/50 mass ratio was found to be the most suitable composition for e.g. high performance coating application.

Department : Chemical Engineering Student's Signature

Field of Study : Chemical Engineering Advisor's Signature

Academic Year : 2012 Co-advisor's Signature.....

ACKNOWLEDGEMENTS

I am sincerely grateful to my advisors, Associate Professor Dr. Sarawut Rimdusit and Associate Professor Dr. Neeracha Sanchavanakit, for their invaluable guidance and suggestions including constant encourage throughout this study. Furthermore, I deeply appreciate all the things. I have learnt from Associate Professor Sarawut and for the opportunity to work in his group. I really enjoyed our meetings and pleasure with my thesis. I am also thankful to Associate Professor Dr. Muenduen Phisalaphong, Associate Professor Seeroong Prichanont and Dr. Phiriyatorn Suwanmala, who have been members of my thesis committee.

In addition, I would like to thank the Dental Material Sciences Research Center, Faculty of Dentistry, Chulalongkorn University for the assistance on micro-hardness testing.

Many appreciations are due to Ms. Kanittha Kamonchaivanich at CPAC Tile Roof Co., Ltd., and Thai Polycarbonate Co. Ltd., for providing materials including urethane acrylate prepolymer and bisphenol A, respectively. Moreover, I gratefully acknowledge Dr. Kasinee Hemvichian of Thailand Institute of Nuclear Technology for her kind assistance on Thermogravimetric Analysis experiment (TGA).

Additionally, I would like to extend my many thanks to all members of Polymer Engineering Laboratory, Department of Chemical Engineering, Faculty of Engineering, Chulalongkorn University, for their assistance, discussion, and friendly encouragement in solving the research problems. Finally, my deepest regard to my parents, who have always been the source of my unconditional love, understanding, and generous encouragement during my studies. Also, every person who deserves thanks for encouragement and support that cannot be listed here.

CONTENTS

	PAGE
ABSTRACT (THAI)	iv
ABSTRACT (ENGLISH)	v
ACKNOWLEDGEMENTS	vi
CONTENTS	vii
LIST OF TABLE	x
LIST OF FIGURES	xi
 CHAPTER	
I INTRODUCTION	1
1.1 Overview	1
1.2 Objectives.....	6
1.3 Scopes of Research	6
 II THEORY	7
2.1 Polyurethane	7
2.2 UV-Curable Polyurethane Acrylate	7
2.3 Benzoxazine Resin.....	8
2.4 Raw Materials.....	11
2.4.1 Synthesis bifunctional benzoxazine monomer based on bisphenol A.....	11
2.4.1.1 Bisphenol A.....	11
2.4.1.2 Formaldehyde.....	12
2.4.1.3 Aniline.....	12
2.5 Interpenetrating polymer networks (IPNs).....	13
2.6 Radiation Curing Process.....	15

	PAGE
III LITERATURE REVIEWS	20
IV EXPERIMENT	34
4.1 Raw Materials	34
4.2 Synthesis of Benzoxazine Monomer	34
4.3 Preparation of Benzoxazine-Urethane Alloys.....	35
4.4 Sample Characterizations.....	35
4.4.1 Fourier Transform Infrared Spectroscopy (FT-IR).....	35
4.4.2 Differential Scanning Calorimetry (DSC).....	35
4.4.3 Dynamic Mechanical Analysis (DMA).....	36
4.4.4 Thermogravimetric Analysis (TGA).....	37
4.4.5 Micro-hardness Tester.....	38
4.4.6 Contact Angle Measurement.....	39
4.4.7 Water Adsorption Measurement.....	40
4.4.8 Water Vapor Transmission Rate Analysis.....	41
V RESULTS AND DISCUSSION	43
5.1 Network Formation of Uretahne Acrylate and Benzoxazine Resin Mixture by Fourier Transform Infrared Spectoscopy.....	43
5.2 Determination of Fully Cured Conditions of PUA/BA-a Alloy Films by PUA/BA-a Alloy Films by Differential Scanning Calorimetry.....	45
5.3 Characterizations of the PUA/BA-a Alloy Films.....	46
5.3.1 Dynamic Mechanical Analysis of the PUA/BA-a Alloy Films.....	46
5.3.1.1 Analysis of Activation Energy (ΔE_a) of Glass Transition Temperature of the PUA/BA-a Film Alloys.....	49
5.3.2 Thermal Degradation of the PUA/BA-a Polymer Alloy Films	50
5.3.3 Hardness Properties of the PUA/BA-a Alloy Films.....	51
5.3.4 Water Absorption Properties of the PUA/BA-a Alloy Films.....	52
5.3.5 Water Contact Angles of the PUA/BA-a Alloy Films.....	52
5.3.6 Water Vapor Transmission Rate of the PUA/BA-a Alloy Films.....	53

	PAGE
VI CONCLUSIONS	70
REFERENCES	72
APPENDICES	80
APPENDIX A Dynamic Mechanical Properties of PUA/BA-a Alloy Films..	81
APPENDIX B Thermal Properties of PUA/BA-a Alloy Films	83
APPENDIX C Mechanical Properties of PUA/BA-a Alloy Films.....	84
APPENDIX D Physical Properties of PUA/BA-a Alloy Films.....	85
VITAE	87

LIST OF TABLE

TABLE	PAGE
3.1 Nomenclature and formulations of samples	24

LIST OF FIGURES

FIGURE	PAGE
1.1 UV curable urethane acrylate coating for roof tile.....	2
1.2 The Epsilon™ benzoxazine family of resins has a unique orange color.....	5
2.1 Basic reaction schemes for urethane formation.....	7
2.2 Synthesis of bifunctional benzoxazine monomer based on bisphenol A.....	10
2.3 Ring-opening polymerization of bifunctionalbenzoxazine.....	11
2.4 Synthesis of bisphenol A.....	11
2.5 Synthesis of aniline by nitrobenzene.....	12
2.6 Synthesis of aniline by phenol.....	13
2.7 Sequential interpenetrating polymer networks.....	14
2.8 Simultaneous interpenetrating polymer networks.....	14
2.9 Electromagnetic energy spectrum.....	16
2.10 Energy as a function of wavelength in comparison to bend energies.....	17
2.11 UV coating from traditional to new applications.....	18
3.1 TGA curves of the BPU/Epoxy IPNs.....	20
3.2 SEM of the BPU/Epoxy IPNs fracture surface.....	21
3.3 Flexural stress and strain of BA-a/PU alloys at various compositions.....	22
3.4 SEM and TEM photographs of IPNs. SEM photographs.....	24
3.5 SEM of the BPU/PF IPNs fracture surface.....	25
3.6 Elongation versus BPU content for BPU/PF IPN.....	26
3.7 Notched izod impact strength versus BPU content for BPU/PF IPNs.....	27
3.8 IR spectra of BA-a, PU prepolymer and PU/BA-a.....	28
3.9 DSC thermograms of PUB/BA-a-90/10 film treated at various temperatures...	29
3.10 TGA analysis of PU/BA-a films.....	30
3.11 DSC thermograms showing the curing exothermic peaks for the fully IPNs....	31
3.12 DSC thermograms of PA/PBZ IPNs at various BA-m compositions.....	32
3.13 The surface free energies and the BA-m contents of the PA/PBZ IPNs.....	33
4.1 Fourier transform infrared spectroscopy analyzer (FTIR).....	35
4.2 Differential scanning calorimetry (DSC).....	36

4.3	Dynamic mechanical analyzer (DMA).....	37
4.4	Thermogravimetric analyzer (TGA).....	38
4.5	Micro-hardness tester model FM-700.....	39
4.6	Contact Angle Analyzer.....	40
4.7	Water Vapor Transmission Rater Analyzer (WVTR).....	42
5.1	FT-IR spectra of benzoxazine resin and polybenzoxazine.....	54
5.2	FT-IR spectra of urethane acrylate prepolymer and polyurethane acrylate.....	55
5.3	FT-IR spectra of PUA/BA-a alloys at 50/50 weight ratio by sequential cure method.....	56
5.4	DSC thermograms of the PUA mixed with BA-a resin at a mass ratio of 50:50 at various curing conditions.....	57
5.5	Storage modulus of PUA/BA-a alloy films at various compositions.....	58
5.6	Crosslink densities of PUA/BA-a alloy films at various compositions.....	59
5.7	Tan δ of PUA/BA-a alloy films at various compositions.....	60
5.8	Photographs of PUA/BA-a alloy films at various composition.....	61
5.9	Height of Tan δ and width at half height of PUA/BA-a alloy films at various compositions.....	62
5.10	DMA curves of PUA/BA-a: 50/50 alloy films at various frequencies.....	63
5.11	Arrhenius plot for the activation energy of the Tg of PUA/BA-a alloy films at various compositions.....	64
5.12	TGA thermogram of PUA/BA-a alloy films at various compositions.....	65
5.13	Hardness of PUA/BA-a alloy films at various compositions.....	66
5.14	Water Absorption of PUA/BA-a alloy films at various compositions.....	67
5.15	Contact angles of PUA/BA-a alloy films at various compositions.....	68
5.16	Permeation rates of PUA/BA-a alloy films at various compositions.....	69

CHAPTER I

INTRODUCTION

1.1 Overview

Polyurethanes are a very large and varied family of incredibly versatile and useful engineering materials. Polyurethane chemistry as well as the chemistry of its related intermediates has been utilized enormously to develop many products in the form of fibers, soft and hard elastomers, foams, adhesives, binders and coatings. In Thailand, this polymer is often used as rigid foam for sound or heat insulation material or as flexible foam for automotive cushion material etc. However, despite the possibility of tailoring their properties according to final expectations, these compounds suffer from some drawbacks, for instance, low resistance to water and polar solvents, and mainly poor thermal stability. Nowadays, improving the thermal stability of polyurethanes can be achieved by e.g. chemical modification with heterocyclic groups or blending with other more stable polymers [1].

Recently, polyurethanes have gathered considerable interests in the applications of coating systems in various fields. Especially, UV curable polyurethane acrylates (PUA) are very attractive materials which combine relatively good mechanical performances (flexibility, abrasion resistance and toughness), high chemical resistance, excellent aesthetic, and adhesion properties [2].

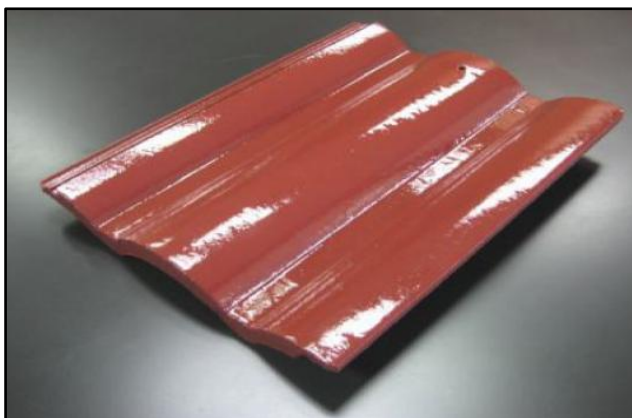


Figure 1.1 UV curable urethane acrylate coating for roof tile [3].

Property improvements of polymeric material by chemical structure modification or blending with other polymers have attracted much attention from material scientists and researchers. Especially, blending method is a relatively simple and fast way in comparison with chemical modification thus gains more interests in industry point of view. One way to combine two different polymer networks together with minimal change of phase separation is by forming the, so called, interpenetrating polymer networks or IPNs.

IPNs are polymer alloys consisting of two or more polymers in a network form which are held together by permanent entanglements with only occasional covalent bonds between the chains of different types of polymers [4]. The obtained network, in some cases, provides excellent thermal stability, good damping properties, and outstanding mechanical properties because of a synergistic effect induced by forced compatibilization of the individual components. For example, **Pandit S.B., and Nadkarni V.M.** [5] successfully synthesized sequential interconnected interpenetrating polymer networks of poly(ester-urethane) and polystyrene by curing at room temperature to complete the PU network formation, followed by a postcure with heat to complete the polymerization of styrene. Their swelling behavior, wide angle x-ray diffraction, and ^{13}C nuclear magnetic resonance were used to examine the IPNs formed in-situ. **Yang J. et al.** [6] prepared polyurethane - polyacrylate interpenetrating networks with three types of urethane-acrylate IPNs, two sequential and one simultaneous. In those IPNs, the urethane was formed under thermal

polymerization, and the acrylate, by photopolymerization. The analysis of glass transition temperature was used to reveal the formation of phase separated domains in the resulting IPNs as a result of varied processing conditions used.

There have been numerous studies on the combinations of urethane and benzoxazine resins for improvement of mechanical properties and thermal stability. For example, **Takeichi T. et al.** [7] reported combinations of polyurethane (PU) that was synthesized from 2,4-tolylene diisocyanate (TDI) and polyethylene adipate polyol (MW ca. 1000) in 2:1 molar ratio and benzoxazine (BA-a). The copolymers show only one glass transition temperature (T_g). The copolymer's T_g was reported to increase with an increase of the BA-a content. Furthermore, thermal stability of the PU was found to be greatly enhanced even with the incorporation of a small amount of BA-a. **Rimduisit S. et al.** [8] reported the comparison of benzoxazine alloying with isophorone diisocyanate (IPDI)-based urethane prepolymers and with flexible epoxy. Alloying with urethane prepolymer was reported to substantially improve the flexibility of the rigid polybenzoxazine. Interestingly, the positive deviation on the glass transition temperature (T_g) of the benzoxazine-urethane alloys was clearly observed, i.e. T_g of the benzoxazine-urethane alloys were significantly greater (T_g beyond 200°C) than those of the parent polymers (T_g of polybenzoxazine = 160°C ; T_g of urethane = -70°C). Moreover, the T_g of benzoxazine-urethane alloy was unexpectedly found to increase with an increase of the softer elastomeric urethane fraction. **Yeganeh H. et al.** [9] improved thermal stability of polybenzoxazine-modified polyurethanes. Their results revealed that thermal stability and flammability of the polymer hybrids were considerably improved in comparison to common thermoset polyurethanes. The degree of improvement was greater with increasing BA-a content. In addition, the BA-a/EPU (50/50 mass ratio) sample had been reported to show the most favored amount of the dissipation factor and the least value of the dielectric constant (DC). The obtained low moisture uptake and excellent solvent resistance of these blends were other fascinating factors that increase the merit of this new class of material for such application as electrical insulators etc.

Polybenzoxazine are a newly developed class of phenolic resins. These novel types of phenolic resins have not only the characteristics of traditional phenolic resins such as excellent thermal properties, flame retardance and high char yield, but also possess unique characteristics such as molecular design flexibility, very low moisture absorption, near zero shrinkage upon polymerization, low melt viscosities, and low dielectric constant. Polybenzoxazine can be synthesized using the patented solventless technology to yield a clean precursor without the need for solvent elimination or monomer purification, which creates serious no threats to environment and human health [10]. Moreover, polybenzoxazine have presently been produced and commercialized in various chemical industries. For example, benzoxazine monomer was scaled-up by Shikoku Chemicals Corporation in Japan and is sold as a chemical reagent [11]. Henkel benzoxazine resin 99110 is claimed by Henkel as a unique resin system which is stable at ambient temperatures for over six months as a one-part resin whereas Epsilon™ composite products from the same company [12] are polybenzoxazine composites suggested for aerospace applications. Major features with related benefits of polybenzoxazine include

- Broad processing window – great for large parts and intricate shapes.
- Low heat release during cure – allows the manufacture of large product parts with lower residual stress.
- Viscosity stability – long injection window for large parts.
- High hot/wet property retention - high service temperatures to enable a wide range of aircraft applications.
- Low cure shrinkage – improved molding ability and strength in final part.
- Fire retardant – suitable for aircraft fuselage and interior applications.
- Improved UV resistance – reduced discoloration compared to epoxies.
- Good thermal resistance – acceptable for high temperature areas.



Figure 1.2 Epsilon™ benzoxazine family of resins has a unique orange color [12].

Note: FST testing = Fire, Smoke, Toxicity testing.

Moreover, Huntsman Advanced Materials recently commercializes 5 grades of Araldite benzoxazine resins with different backbones based on bisphenol A, bisphenol F, phenolphthalein, thiodiphenol, and dicyclopentadiene. Several products have been developed for laminating and structural composite applications with growing trend in electronic applications. In addition, benzoxazine resins are also promising candidates for composites, coatings, adhesives, and encapsulants among others due to their excellent performance such as high temperature resistance, dimensional stability, low water absorption, low dielectric constant, good thermomechanical properties, and flame retardancy [13].

Currently there is no report on characteristics of urethane acrylate-benzoxazine hybrid polymer networks. Therefore, the objective of this research is to investigate the formation of polymer hybrids between the two resins cured under different mechanisms and to evaluate properties of the UV curable polyurethane acrylate by alloying with the thermal curable benzoxazine resin. The sequential curing methods are used for sample preparation in order to retain the properties of the two starting polymers i.e. by UV cure followed by thermal cure. Essential chemical, physical, mechanical and thermal properties of the resulting hybrid polymer networks are to be investigated in our work.

1.2 Objectives

1. To study the synthesis and characteristics of sequential interpenetrating polymer networks of polyurethane acrylate and polybenzoxazine.
2. To investigate the effect of polybenzoxazine contents on mechanical and thermal properties of the sequential interpenetrating polymer network based on polyurethane acrylate.

1.3 Scopes of Research

1. Synthesis of benzoxazine resin by solvent less synthesis technology.
2. Preparation of sequential interpenetrating polymer network of polyurethane acrylate and polybenzoxazine at various weight ratios of urethane acrylate prepolymer and benzoxazine resins i.e. 100:0, 90:10, 80:20, 70:30, 60:40 and 50:50.
3. Evaluation of the curing and crosslink behaviors of the sequential interpenetrating polymer networks of polyurethane acrylate and polybenzoxazine.
4. Examination of chemical, mechanical, thermal and physical properties of sequential interpenetrating polymer network of polyurethane acrylate and polybenzoxazine.
 - Fourier Transform Infrared Spectroscopy (FTIR).
 - Differential Scanning Calorimeter (DSC).
 - Dynamic Mechanical Analyzer (DMA).
 - Thermal Gravimetric Analyzer (TGA).
 - Micro-hardness Tester.
 - Contact Angle Analyzer.
 - Water Vapor Transmission Rate (WVTR)

CHAPTER II

THEORY

2.1 Polyurethanes

Polyurethanes are polymers that have a molecular backbone containing carbamate groups (-NHCOO). These groups, called urethane, are produced through a chemical reaction between a diisocyanate and a polyol (Figure 2.1). First developed in the late 1930s, polyurethanes are some of the most versatile polymers. They are used in building insulation, surface coatings, adhesives, solid plastics, elastomer and athletic apparel.

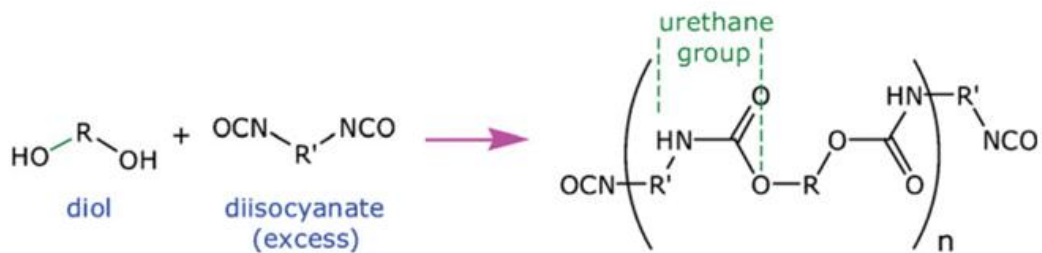


Figure 2.1 Basic reaction schemes for urethane formation [14].

It is apparent that this reaction leads to polyurethane when multifunctional reactants are used. When a diisocyanate and a diol react together, linear polyurethane is obtained whilst a diisocyanate and a polyhydric compound (polyol) interaction will lead to a cross-linked polymer [15]. Polyurethane has excellent flexibility, outstanding weathering resistance, high abrasion resistance but low resistance to moisture and poor thermal stability. Polyurethane is used in many applications such as automotive, furniture, construction, thermal insulation, biopolymer and sportswear [16].

2.2 UV-curable Polyurethane Acrylate

Poly(urethane acrylate) can potentially combine the high abrasion resistance, toughness, tear strength, and good low temperature properties of polyurethane with

the good optical properties and weather ability of the polyacrylate. In poly(urethane acrylate) system, the polyurethane backbone may contain polyether or polyester soft segment, diisocyanate hard segment, and acrylate pendant group, which are highly responsive to radiation.

The low viscosity liquid oligomers possess excellent process ability while the cured solid polymers have reasonable mechanical strength and good thermal stability due to their crosslink nature. Polymers containing acrylate or methacrylate pendant groups are candidates for radiation sensitive solid polymers since the acrylate groups may undergo crosslinking reactions under suitable conditions [17, 18].

The microphase-separated morphology between the soft and hard segments of the polyurethane provides initial mechanical strength, while further crosslinking can enhance mechanical properties especially at higher temperatures. As a result of their high mechanical strength, flexibility, fatigue resistance and biocompatible nature, polyurethanes have been proven to be potential candidates as biomaterials for e.g. artificial organs [19, 20].

2.3 Benzoxazine Resin

These one-component resins, belonged to the addition cure phenolic family, were developed to combine the thermal properties and flame retardance of phenolics and the mechanical performance and molecular design flexibility of advanced epoxy systems.

Polybenzoxazines overcome several shortcomings of conventional novolac and resole-type phenolic resins, while retaining their benefits. As a result, benzoxazine resins are expected to replace traditional phenolics, polyesters, vinyl esters, epoxies, bismaleimides, cyanate esters and polyimides in many respects. The molecular structure of polybenzoxazine offers superb design flexibility that allows properties of the cured material to be controlled for specific requirements of a wide variety of individual requirements. The physical and mechanical properties of these new polybenzoxazines are exhibited to compare very favorably with those of

conventional phenolic and epoxy resins. The resin permits development of new applications by utilizing some of their unique features such as [21].

- Near zero volumetric change upon polymerization
- Low water absorption
- Fast mechanical property build-up as a function of degree of polymerization
- High char-yield
- Low coefficient thermal expansion
- Low viscosity
- Excellent electrical properties

However, there are some inherent shortcomings for polybenzoxazines. These include the brittleness of the cured resin, which is a common problem for thermosets. A relatively high temperature (ca. 200°C) needed for the ring-opening polymerization, or curing reaction, although acidic catalyst is effective to lower the cure temperature. Another shortcoming is the difficulty to process into thin film from the typical monomers because most monomers are powder at room temperature and possess very low a-stage viscosity while the cured polymers are brittle [19].

Benzoxazine resins are typically synthesized using phenol, formaldehyde and amine (aliphatic or aromatic) as starting materials either by employing solution or solventless methods. They can be synthesized using various phenols and amines with different substitution groups attached [24]. The patented solventless technology provides a clean benzoxazine precursor without the need for solvent elimination or monomer purification, which creates no serious threats to environment and human health [23].

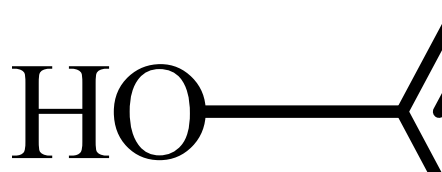
In this work, we synthesize bifunctional benzoxazine monomer which prepared from bisphenol-A, formaldehyde, aniline (Figure 2.2) [25]. Upon heating, bi-functional benzoxazines form a high molecular weight polymer via a ring opening mechanism (Figure 2.3). It has been proposed that, the ring-opening initiation of

benzoxazine results in the formation of a carbocation and an iminium ion which are in equilibrium [26]. Polymerization proceeds via the electrophilic substitution by the carbocation to the benzene ring. This transfer occurs preferentially at the free ortho and para position of the phenol group. The stability of the iminium ion greatly affects the propagation rate because carbocation is responsible for propagation. However, several authors have proposed different other mechanisms of thermal curing of benzoxazine resin [27].

Bisphenol

Formaldehyde

Aniline



BA-a benzoxazine monomer

Figure 2.2 Synthesis of bifunctional benzoxazine monomer based on bisphenol A.

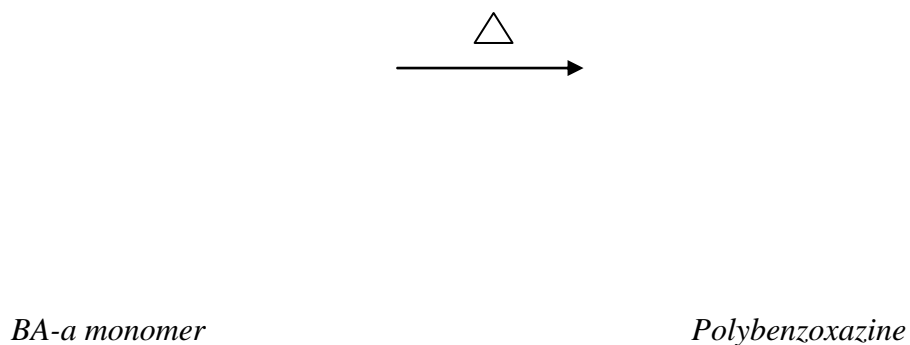


Figure 2.3 Ring-opening polymerization of the bifunctional benzoxazine resin [7].

2.4 Raw Materials

2.4.1 Synthesis of bifunctional benzoxazine monomer based on bisphenol A

2.4.1.1 Bisphenol A

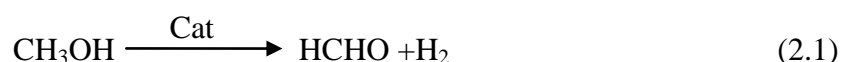
Bisphenol A is produced by reacting phenol with acetone in a presence of an acid catalyst (Figure 2.4). Common catalysts are aqueous acids or acid clays. Promoters such as thioglycolic acid and resorcinol can also be used [26].



Figure 2.4 Synthesis of bisphenol A.

2.4.1.2 Formaldehyde

Formaldehyde is an unstable colorless gas, which is commercially supplied in 37% aqueous solution, as a solid cyclic trimer (trioxan), and as a solid polymer (para-formaldehyde) which is used in this work. Almost all formaldehyde produced is derived from methanol either by oxidative dehydrogenation using silver or copper catalyst (Equation 2.1) or by oxidation in the presence of Fe_2O_3 and MoO_3 (Equation 2.2) [28].



In the oxidative dehydrogenation, the generated hydrogen is oxidized to water upon addition of air.



2.4.1.3 Aniline

The classical method of synthesis of aniline is the reduction of nitrobenzene with hydrogen in the vapor phase using a copper/silica catalyst (Figure 2.5). Nitrobenzene is produced in the nitration of benzene using a mixture of nitric acid and sulfuric acid.

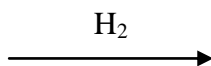


Figure 2.5 Synthesis of aniline by nitrobenzene.

Recently, Aristech Chemical completed a 90,000-ton aniline plant using plant using phenol as the feedstock. This technology was developed by Halcon, and it is

also used by Mitsui Toatsu in Japan. The amination of phenol is conducted in the vapor phase using an alumina catalyst with very high yields.



Figure 2.6 Synthesis of aniline by phenol.

2.5 Interpenetrating Polymer Networks (IPNs)

An interpenetrating polymer network (IPN), belonged to a unique class of polymer blends or alloys, consists of two or more distinct crosslink polymer networks held together by permanent interpenetration. IPNs are highly attractive materials since they allow the combination, in network form, of two otherwise incompatible polymers. This characteristic structure of IPNs sometimes results in synergistic effect on properties, which is suggested to combine good properties of different polymer networks [29]. The resulting properties are strictly related to both the chemical structure of the networks and the synthesis path of the IPNs. In practice, two main synthesis routes are often used:

(i) Sequential IPNs, where polymer network I is prepared first. Network I swells in monomer II and cross-linking agent and is then polymerized in situ. Thus, in sequential IPNs the synthesis of one network follows the synthesis of the other (Figure 2.7).

(ii) Simultaneous IPNs, where the monomers or prepolymers and cross-linking agents for synthesis of both networks are mixed together. The reactions are carried out simultaneously. It is important that the cross-linking reaction should proceed according to different mechanisms to avoid chemical interaction between macromolecules of the two networks. Usually these mechanisms are polyaddition and radical polymerization (Figure 2.8).

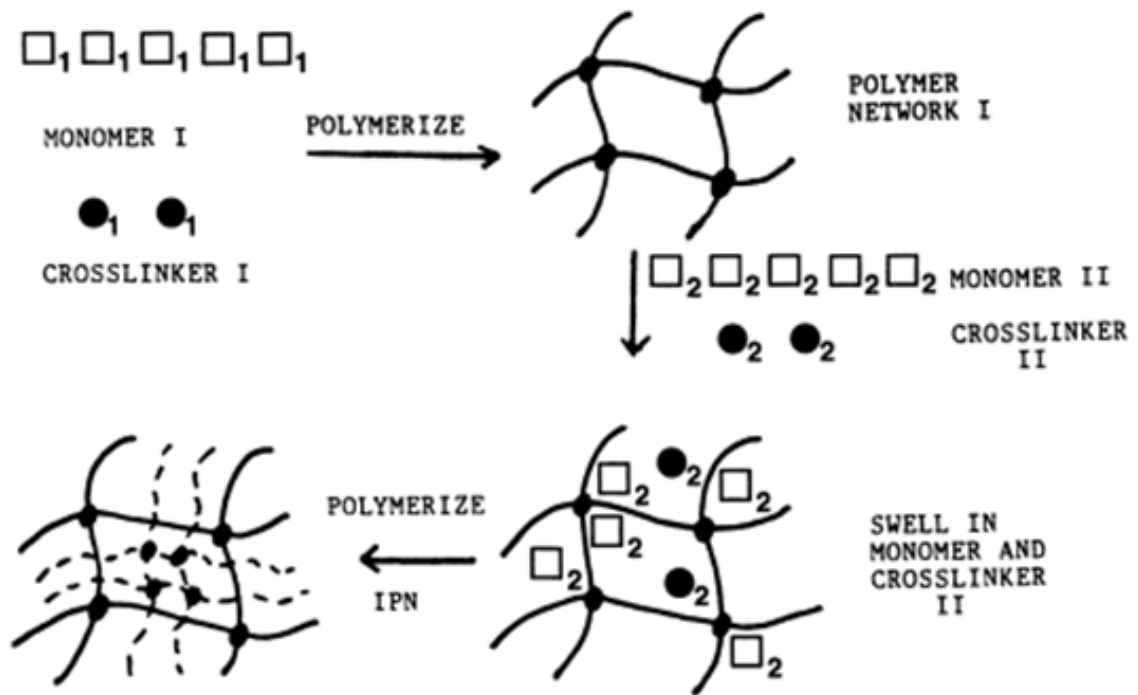


Figure 2.7 Sequential interpenetrating polymer networks [30]

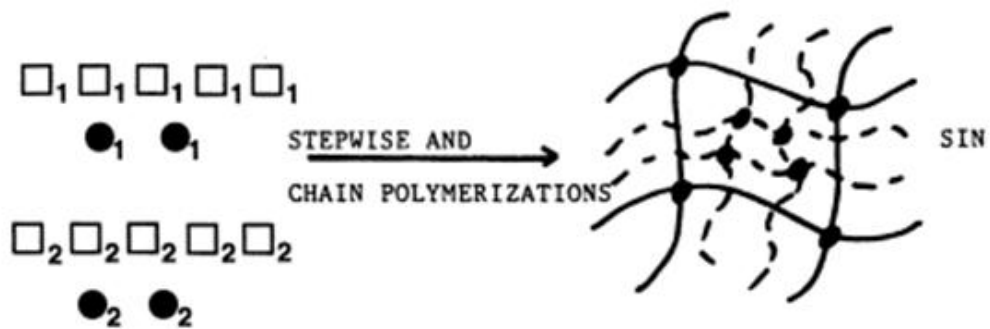


Figure 2.8 Simultaneous interpenetrating polymer networks [30]

In cases (i) and (ii), chain transfer via polymerization may take place and grafted IPNs may be formed. Another very important class of IPNs is semi-IPNs, namely, systems in which one of the components is a linear polymer. Semi-IPNs may be characterized as sequential or simultaneous IPNs depending on the way the linear polymer is introduced. Various types of IPNs may also be classified by the mechanism of phase separation proceeding during IPN formation. These mechanisms are nucleation and growth, and spinodal decomposition. Differences in the conditions

of phase separation predetermine the physical and morphological features of IPNs [30].

2.6. Radiation Curing Process

UV curing has now been established as an alternative curing mechanism to thermal hardening, contrary to the past, where it was only considered for the curing on temperature sensitive substrates, like wood, paper and plastics. This alternative curing technology uses energy of photons of radiation sources in the short wavelength region of the electromagnetic spectrum in order to form reactive species, which trigger a fast chain growth curing reaction. Out of the electromagnetic spectrum (shown in Figure 2.9) is the range from the near infrared (NIR), over visible and ultraviolet (UV) to electron beams and X-ray, the UV region, which is further classified into UV-A, UV-B, and UV-C radiation, is mainly used for this technology [31].

The energy content of a photon is defined by the equation

$$E = h\nu = hc/\lambda \quad (2.3)$$

Where ν is the frequency and λ is the wavelength (nm). This equation tells us, that the shorter the wavelength, the higher the energy of a photon. UV light, in the wavelength region of 300–400 nm, should already be able to cleave C–C bonds. The high energy photons of e-beam and X-ray are sufficient to cleave C–C or C–H bonds, thus, they do not need a special photo initiator for forming the desired radical species as initiators for polymerization. In the case of UV exposure, however, photo initiators are commonly used since the direct cleavage processes are not efficient enough. The photo initiators are excited and, after a cascade of reactions, form the desired reactive species. In the case of using longer wavelength exposures, more complicated energy transfer reactions are needed [31].

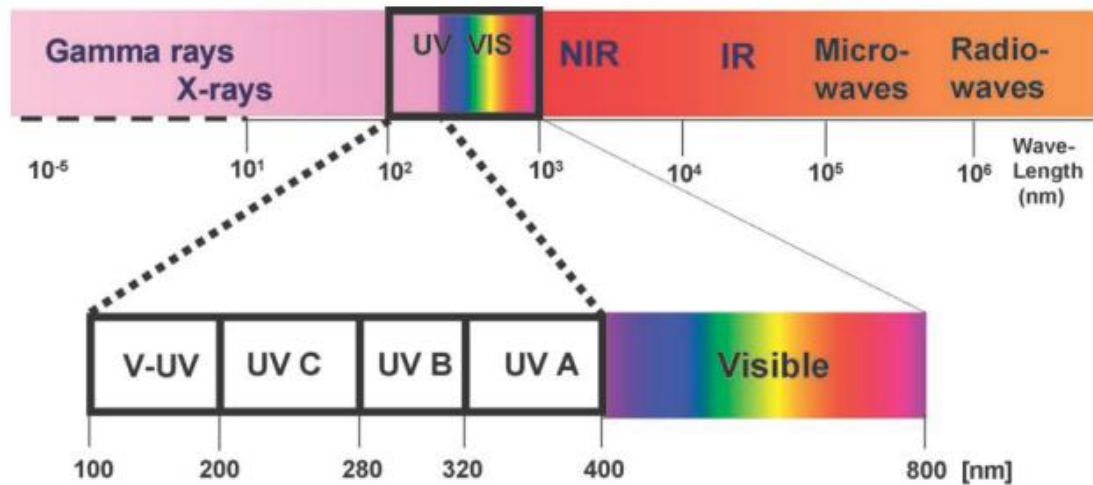


Figure 2.9 Electromagnetic energy spectrums [31].

From the spectrum of usable radiation energy sources, UV technology is by far the most common one. From the higher energy radiation sources, e-beam technology has been widely explored for coatings technologies. It is still the most economical technology for industrial applications with very high volumes. However, the high safety requirements related to the use of e-beam technology and the high investment costs hamper the wide spreaduse of this technology. At the Rad Tech Conference 2005 in Barcelona, considerable interest has been expressed in the session dealing with e-beam technology for printing, varnishing and laminating for the packaging industry [32]. The reasons for this alertness are new developments of compact and less expensive e-beam equipment and new formulation advances in flexographic printing inks, coatings and adhesives. Especially in the packaging printing for food contact applications, the use of EB technology has advantages over UV coatings since no photoinitiator is needed, which can migrate, if the coating is inadequately cured.

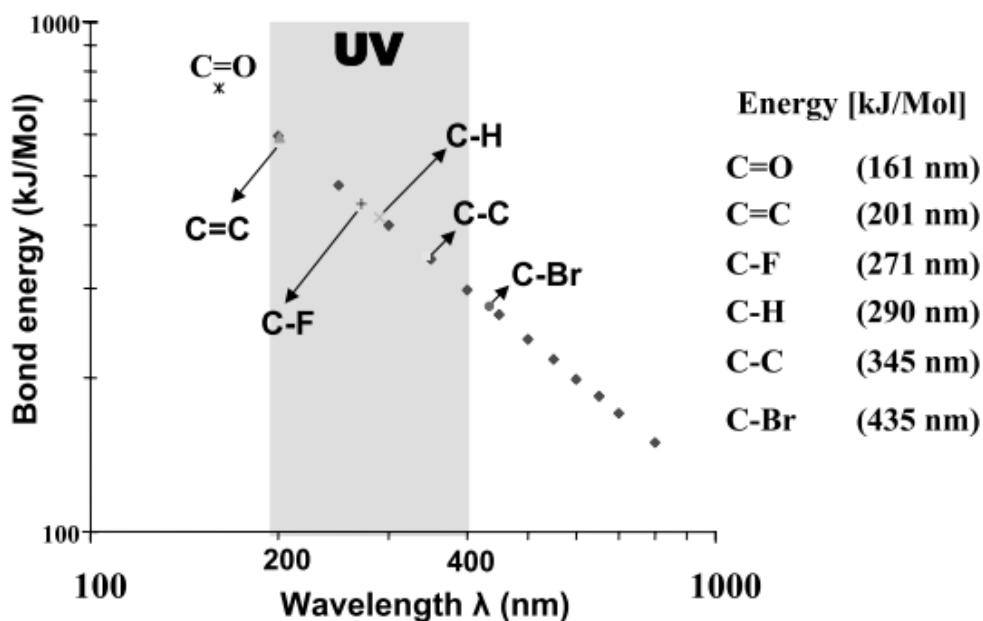


Figure 2.10 Energy as a function of wavelength in comparison to bond energy [31].

As can be seen from the few example applications shown in Figure 2.11, UV curable coatings are traditionally used on temperature sensitive substrates, like wood, paper and plastics, for example, clear coats for parquet, furniture, vinyl flooring, on plastic substrates (crash helmet, boards), compact discs, headlight lenses or overprint varnishes (posters, high gloss packaging). However, since coatings are used almost everywhere, the UV coating market is expanding to new applications, where traditionally thermal curing systems have been the workhorses. Applications like UV curable coatings on metals (automotive, coil coating) and exterior uses on windows, on glass, bikes, on appliances, like refrigerators, washing machines, and most prominently on cars are good examples. A multiplicity of coating applications is often less noticed, such as adhesives and protective coatings for DVD and CD's, protective coating on glass fiber wires, inside and outside of beverage cans, on automotive parts, like headlight mirrors and in multiple functions on electronic parts. This list can easily be extended even further.

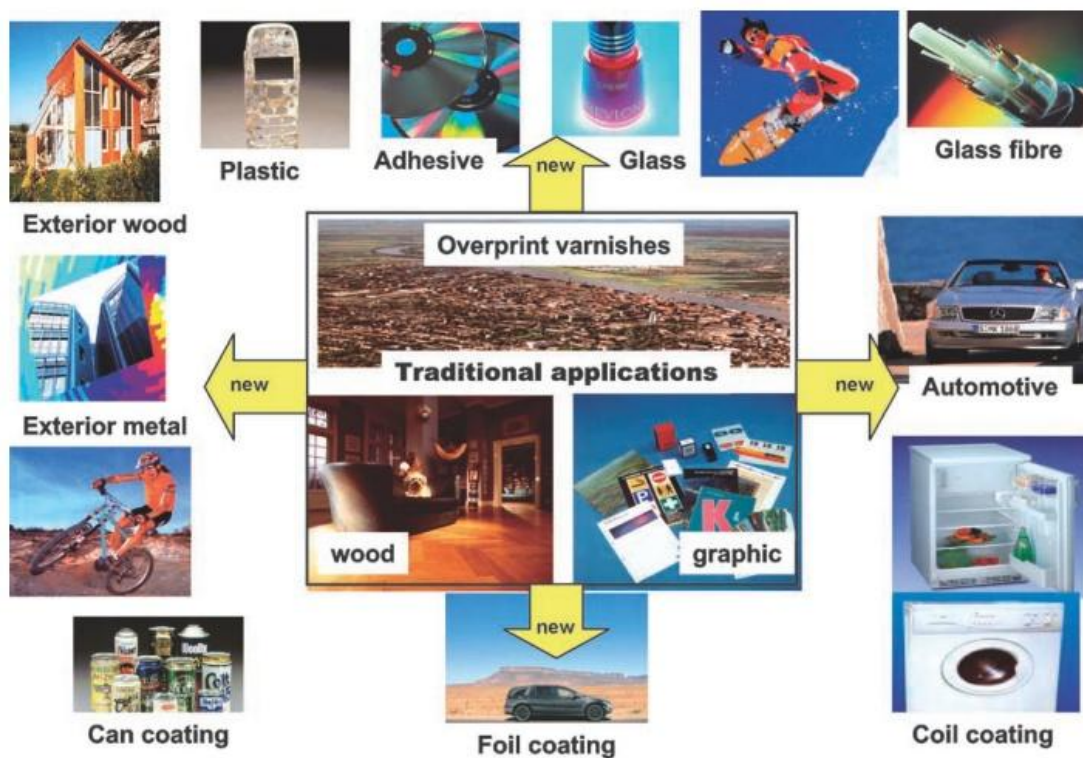


Figure 2.11 UV coatings – from traditional to new applications [31].

The UV curing process requires a light source which directs UV or visible light onto the formulated product. Photoinitiators absorb the UV energy from the light source, setting in motion a chemical reaction that quickly, in fractions of a second, converts the liquid formulation into a solid, cured film. The bulk of the formulation is made up of monomers and oligomers. Monomers are low molecular weight materials. They can be mono or multifunctional molecules, depending on the number of reactive groups (usually acrylate) they possess. Functional monomers become part of the polymer matrix in the cured coating because their reactive functional groups undergo polymerization during exposure to UV light [33].

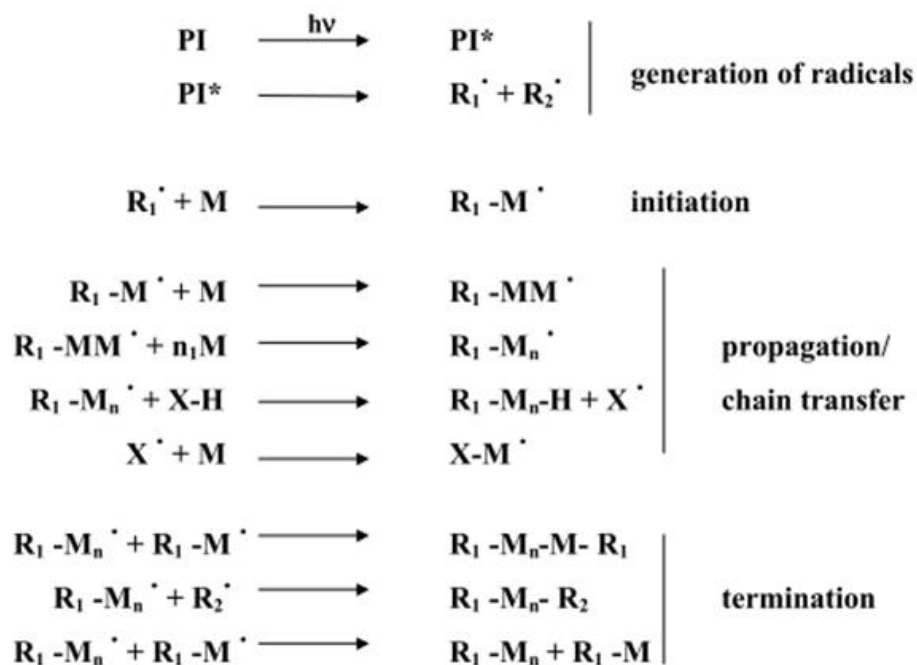
Monomers also function as diluents in the formulations, used to adjust system viscosity, and are sometimes referred to as reactive diluents. Oligomers, conversely, tend to be of higher molecular weight, viscous materials where the molecular weight ranges from several hundred to several thousand grams/mole or even higher. Usually, the type of oligomer backbone determines the final properties of the coating such as

flexibility, toughness etc. These backbones can be epoxy, polyether, polyester, polyurethane or other types. The functional groups that provide linkages between molecules are located at both ends of the oligomer molecules. The functionality that is found to be most effective is the acrylate functional group.

The photoinitiator is the key of the curing process because it starts polymerization and crosslinking reaction. Under UV irradiation the photoinitiator fragments into free radicals that are the reactive species for the polymerization of unsaturated moieties [31].

The curing process develops through the following steps:

- Generation of the reactive species (radicals)
- Initiation
- Propagation/chain transfer
- Termination



CHAPTER III

LITERATURE REVIEWS

Chen, C.H. and Chen, M.H. (2006) [4] investigated an interpenetrating polymer network synthesis of blocked PU and epoxy resins using simultaneous polymerization method. Thermal properties and morphology of blocked PU/epoxy full interpenetrating polymer network (full-IPN) which were prepared from blocked NCO-terminated PU prepolymer with chain extender, and epoxy prepolymer, with curing agent. The weight loss monitored from thermogravimetric analysis (TGA) of the IPN at various blocked PU/epoxy IPN compositions i.e. 0/100, 35/65, 50/50, and 100/0 is displayed in Figure 3.1. From the figure, degradation temperature defined at the weight loss of 10% of the full-IPNs decreased with increasing the blocked PU content. The thermal degraded temperatures of the IPNs were reported to be 367, 355, 301 and 281°C, respectively.

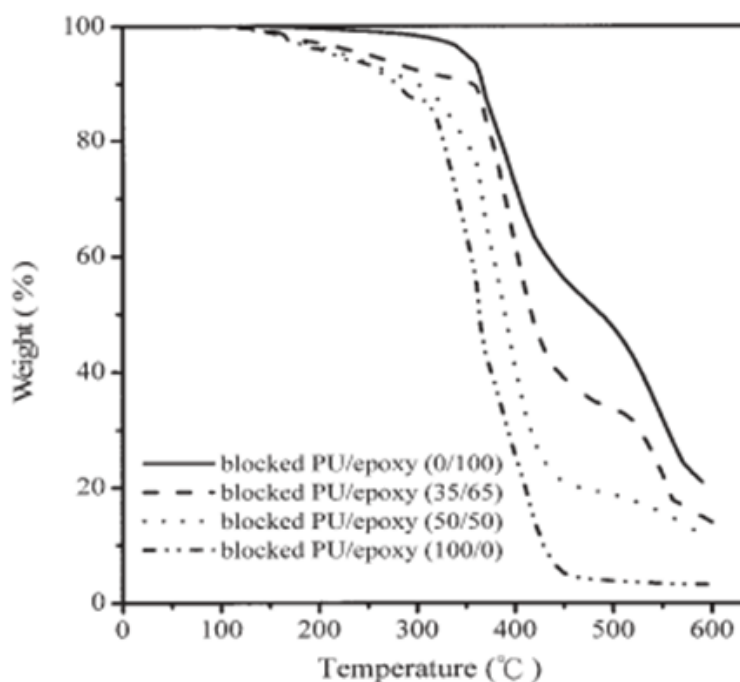


Figure 3.1 Weight loss by TGA versus temperature of the blocked PU/epoxy IPN at various blocked PU contents [4].

Figure 3.2 shows the scanning electron micrographs of fracture surface of the blocked PU/epoxy IPN at various blocked PU contents. From the figure, the rougher fracture surface was observed when the amount of the blocked PU in the epoxy increased. In the Figure 3.2(a), the pure epoxy, a brittle material, exhibited smooth and glossy microstructure whereas the fracture surface of the blocked PU revealed the rough microstructure as they are flexible materials as shown in Figure 3.2(e). For the IPN system (Figure 3.2(b)-(d)), the microstructure of the IPNs became rougher.

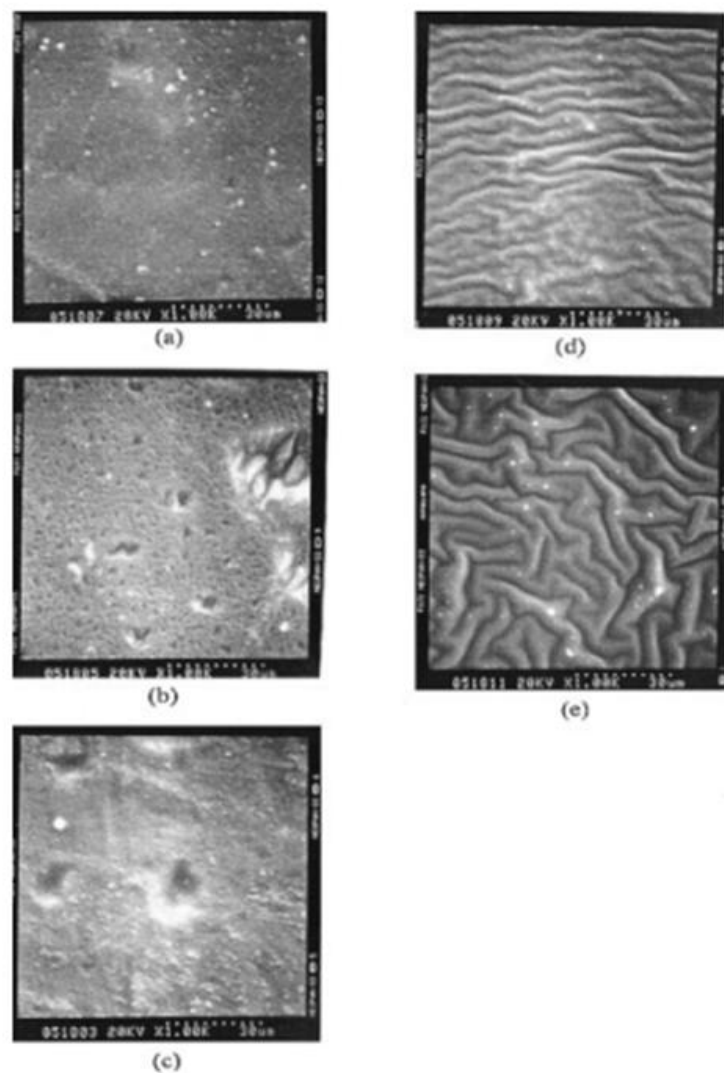


Figure 3.2 Scanning electron micrographs (SEM) of fracture surface of the blocked PU/epoxy IPN at various blocked PU contents: (a) 0/100, (b) 25/75, (c) 50/50, (d) 75/25, (e) 100/0 [4].

Rimduisit, S., Pirstpindvong, S., Tanthapanichakoon, W. and Damrongsakkul, S. (2005) [8] reported improved toughness of bisphenol-A and aniline based polybenzoxazine (PBA-a) by alloying with urethane prepolymer (PU) synthesized from isophoronediiisocyanate(TDI) and polyester polyol (MW ca. 2000) in 2:1 molar ratio. The authors found that glass transition temperatures (T_g s) of the BA-a/PU alloys are significantly higher (T_g beyond 200°C) than those the parent polymers, PBA-a and the PU, i.e., 165°C and -70°C, respectively.

In addition, the effects of the PU contents on the flexural properties of the alloys are shown in Figure 3.3. From the figure, the flexural strength of the BA-a/PU at a weight ratio of 90/10 was slightly higher than that of the neat PBA-a. The flexural strength then decreased as the mass fraction of the PU increased beyond 20 wt%. Importantly, the incorporation of the PU into the PBA-a was found to lower the flexural modulus of these alloys monotonically whereas the toughness of the BA-a/PU increased with the mass fraction of the PU.

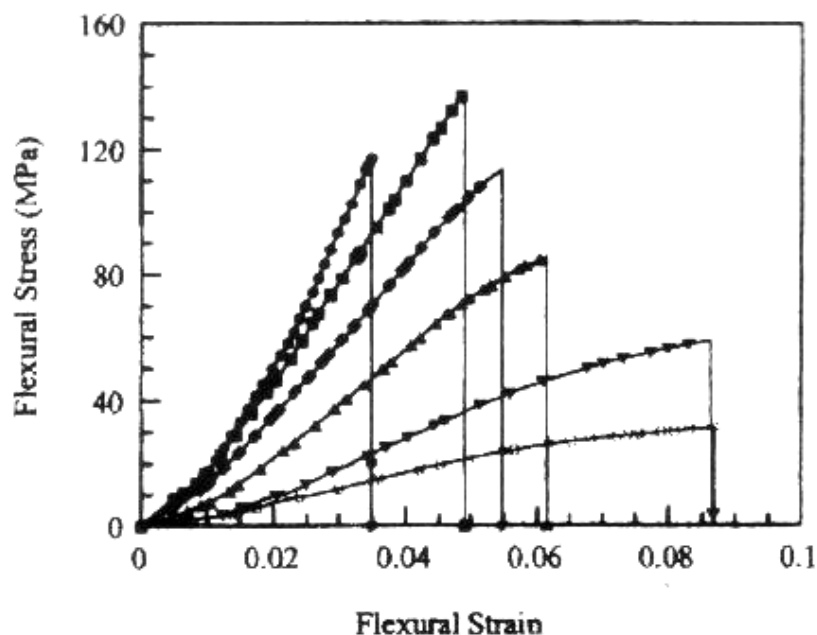


Figure 3.3 Flexural stress and strain of BA-a/PU alloys at various compositions: (●) 100/0, (■) 90/10, (◆) 80/20, (▲) 70/30, (▼) 60/40 and (●) 50/50 [8].

Cui, Y., Chen, Y., Wang, X., Tian, G. and Tang, X. (2003) [33] prepared polyurethane/polybenzoxazine-based interpenetrating polymer networks (IPNs) from a benzoxazine monomer (BA-a) and polyurethane synthesized from diphenylmethanediisocyanate (MDI), poly(ethylene glycol) (PEG) with an average molecular weight 1000 g mol^{-1} , 1,4-butanediol (BD) and 1,1,1-trimethylolpropane (TMP). The nomenclature of the samples is listed in Table 3.1. The FTIR spectra of the resulting PU/PBA-a IPNs indicate that all bands in the spectrum can be found in that of the each component polymer. Therefore, it is inferred that there are no apparent graft reaction between the two component networks during the formation of IPN.

Figure 3.4 shows the surface morphology using scanning electron micrograph (SEM) of the PU/PBA-a IPNs with different compositions. Although exhibiting a transparent appearance, the PU/PBA-a IPNs showed phase separation to a certain level regardless of composition. By comparing, the phase size of the PBA-a in the lower tri-functional cross linker formed PU-based IPN (Figure 3.5(a)-(b)) is higher than in the more crosslink PU-based IPN. The difference observed between another series of the PU/PBA-a ratios (Figure 3.4(c)-(d)) well confirms this change. Moreover, the surface morphology using transmission electron microscopy (TEM) in Figure 3.4(e)-(f) similarly displayed to that observed from SEM. From the figures, two networks exhibit good entanglement and interpenetrating behavior as expected. The size of the PBA-a network, the dark phase, decreased with increasing the PU composition

Table 3.1 Nomenclature and formulations of samples.

Sample code	MDI/PEG/BD/TMP/ by molar ratio	PU/PBa by weight
PBa	-	0/1
PU 10	3.05/1/1.8/0.2	1/0
PU 10-50	3.05/1/1.8/0.2	1/1
PU 10-66	3.05/1/1.8/0.2	2/1
PU 10-75	3.05/1/1.8/0.2	3/1
PU 20-50	3.05/1/1.6/0.4	1/1
PU 20-75	3.05/1/1.6/0.4	3/1

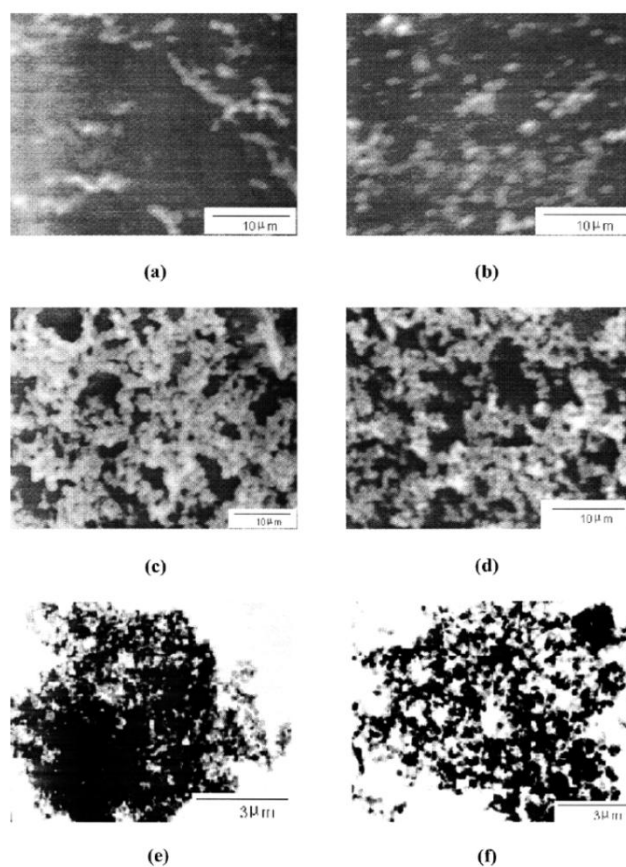


Figure 3.4 SEM and TEM photographs of IPNs. SEM photographs:(a) PU10-75, (b) PU20-75, (c) PU10-50, (d) PU20-50. TEM photographs: (e) PU 10-50, (f) PU20-50 [33].

Sun, Y.Y., and Chen, C.H.(2011) [34] examined interpenetrating polymer networks (IPNs) based on blocked polyurethane (BPU) and phenolic (PF) using a simultaneous polymerization method. The IPN was prepared from BPU prepolymer with *m*-xylylenediamine as a chain extender and PF prepolymer using *p*-toluene sulfonic acid as a catalyst.

Figure 3.5 shows scanning electron micrographs of fracture surface of the pure components of PF and BPU and of BPU/PF IPNs at various BPU contents. From the micrographs, the pure PF expressed smooth and glossy microstructure as it was a brittle material (Figure 3.5a). The BPU, however, exhibited rough microstructure because of its ductile nature (Figure 3.5f). Figure 3.5(b–e) revealed that, as the BPU content of the BPU/PF IPN increased, the microstructure of IPN became rougher. As the BPU content was above 50 wt%, the microstructure is very similar to that of the pure BPU component. It was also found that the BPU was dissolved in the PF of the BPU/PF IPNs. The morphological study suggested that the IPN system was heterogeneous and more than one phase existed in the networks.

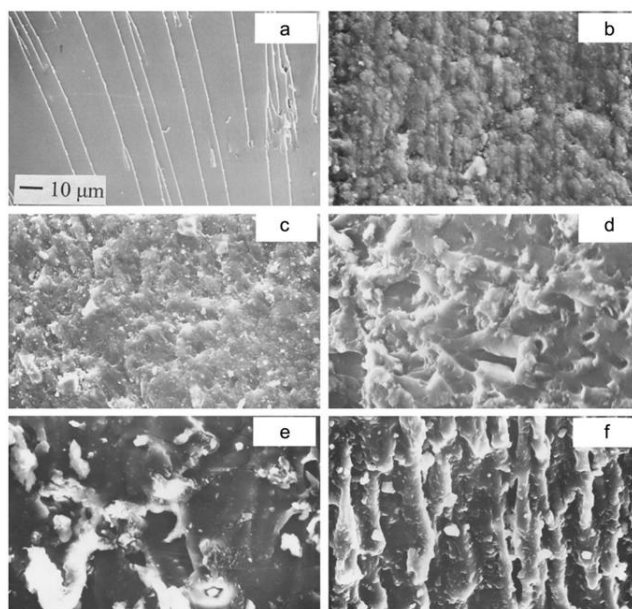


Figure 3.5 Scanning electron micrographs (SEM) of fracture surface of the BPU/PF IPN of (a) 0/100, (b) 15/85, (c) 25/75, (d) 50/50, (e) 75/25 and (f) 100/0 [34].

The elongation and notched izod impact strength versus BPU content for BPU/PF IPNs are shown in Figure. 3.6 -3.7. Because BPU might be partially dissolved in the PF matrix (as can be seen from the SEM photographs) and the interpenetration effect will toughen the matrix of the BPU/PFIPNs, the elongation and notched izod impact strength of the BPU/PF IPNs increased with increasing the BPU content. From these results, it was found that, although there is no rubber particle in the matrix, the notched izod impact strength (i.e., high shear rate in fracturing) still could be improved. The reason is that the soft segment content of the BPU matrix was toughened by the interpenetration effect thus showed an increase in notched izod impact strength. The ductility of the BPU matrix played a very important role in toughening at high shear rate fracturing (i.e., notched izod impact strength).

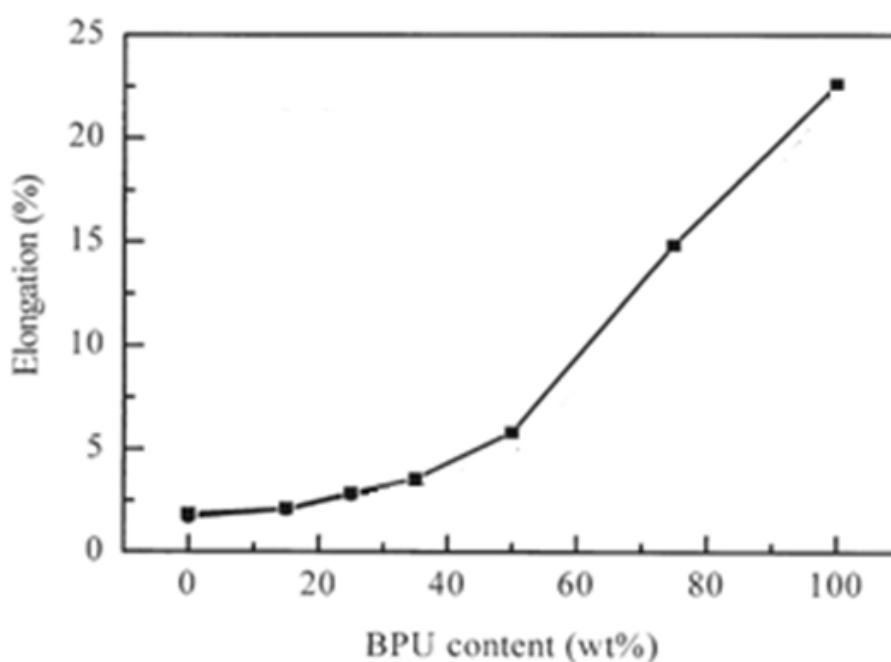


Figure 3.6 Elongation versus BPU content for BPU/PF IPNs[34].

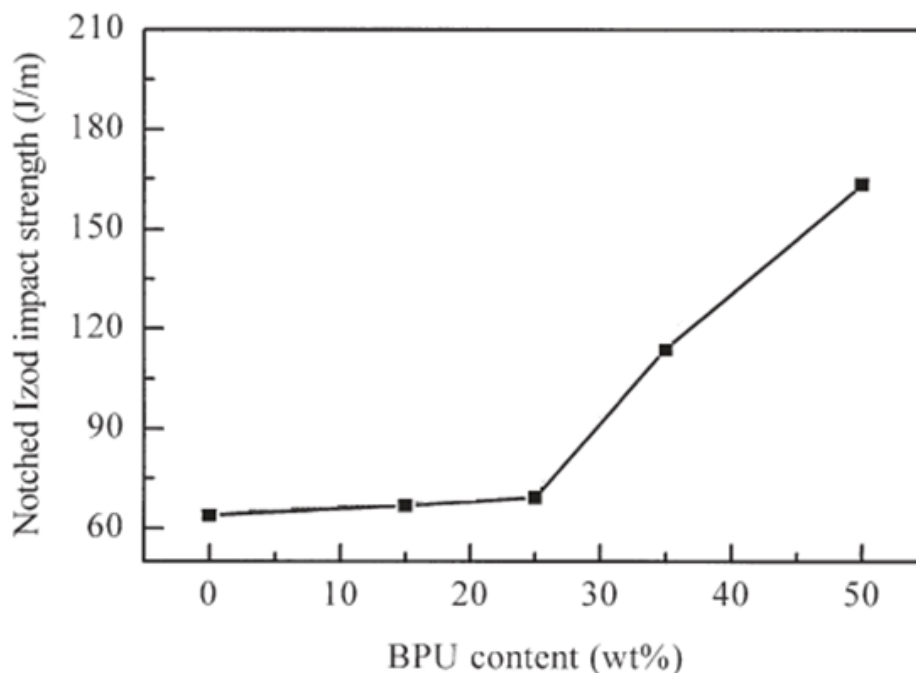


Figure 3.7 Notched Izod impact strength versus BPU content for BPU/PF IPNs[34].

Takeichi, T., Guo, Y. and Agag, T.(2000) [7] prepared poly(urethane-benzoxazine) films as novel polyurethane/phenolic polymer hybrids from blending benzoxazine monomers (Ba) and urethane prepolymers(PU) that was synthesized from 2,4-tolulene diisocyanate(TDI) and polyethylenadipatepolyol(MW ca. 1000) in 2:1 molar ratio.

The progress of the curing of PU/BA-a films was followed by infrared spectroscopic technique. Figure 3.8 shows spectra taken from PU/BA-a films at each curing stage, along with the spectrum of BA-a (Figure 3.8a) and PU prepolymer (Figure 3.8b). All the characteristic absorbanceis clearly observed in PU/BA-a films treated at 100 °C for 1 hr (Figure 3.8c). It is obviously noticed that the disappearance of absorbance at 2275 cm^{-1} after 150 °C/1 hr cure cycle (Figure 3.8d), indicating the reaction of NCO groups in the PU prepolymer. Moreover, the absorptions at 948 cm^{-1} and 1499 cm^{-1} assigned to the tri-substituted benzene ring in BA-a have been weakened with the curing progress, indicating the progress of the ring-opening polymerization reaction of the benzoxazine monomers.

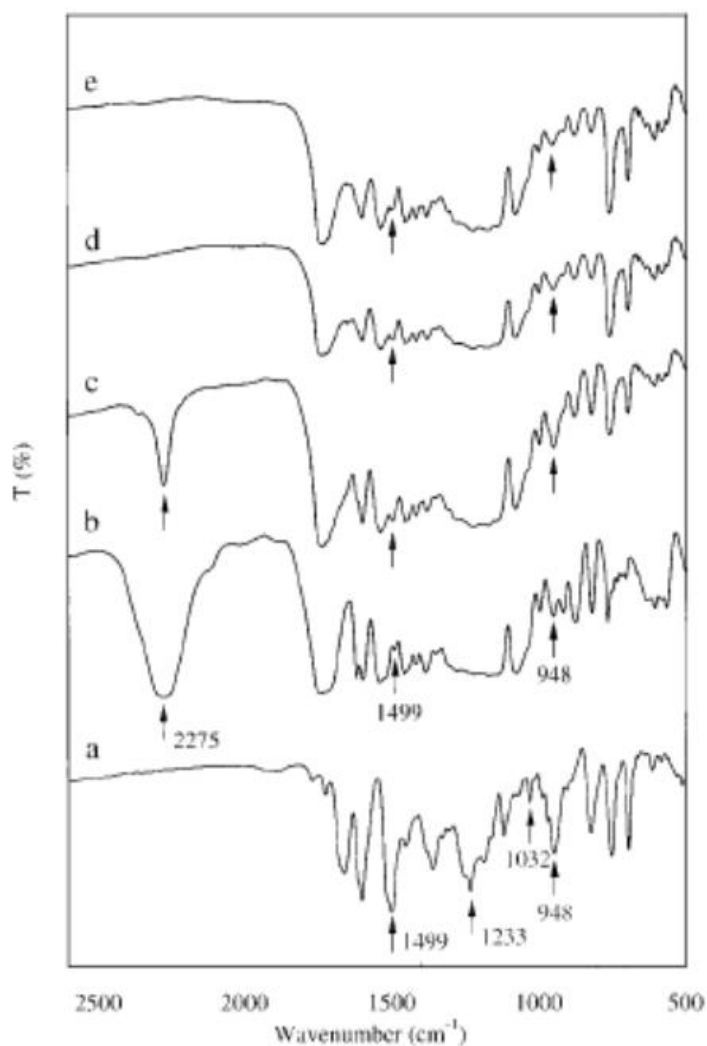


Figure 3.8 IR spectra of: (a) BA-a; (b) PU prepolymer; and PU/BA-a 85/15 Treated at: (c) 100 °C/1 hr, (d) 150 °C/1 hr and (e) 190 °C/1 hr[7].

For more investigation of the curing behavior of benzoxazine monomers in the presence of the PU prepolymers, DSC measurement was recorded. Examples of DSC results are shown in Figure 3.9 in the case of PU/BA-a (90/10). Exotherm due to the ring opening of BA-a is clearly seen in this figure. The exothermic curing enthalpy upon curing decreases from 6.2 cal/g to 3.8 cal/g as the curing temperature is increased from 100 °C to 150 °C, suggesting that the partial ring-opening of BA-a occurs at 150 °C, affording polybenzoxazine containing phenolic OH groups.

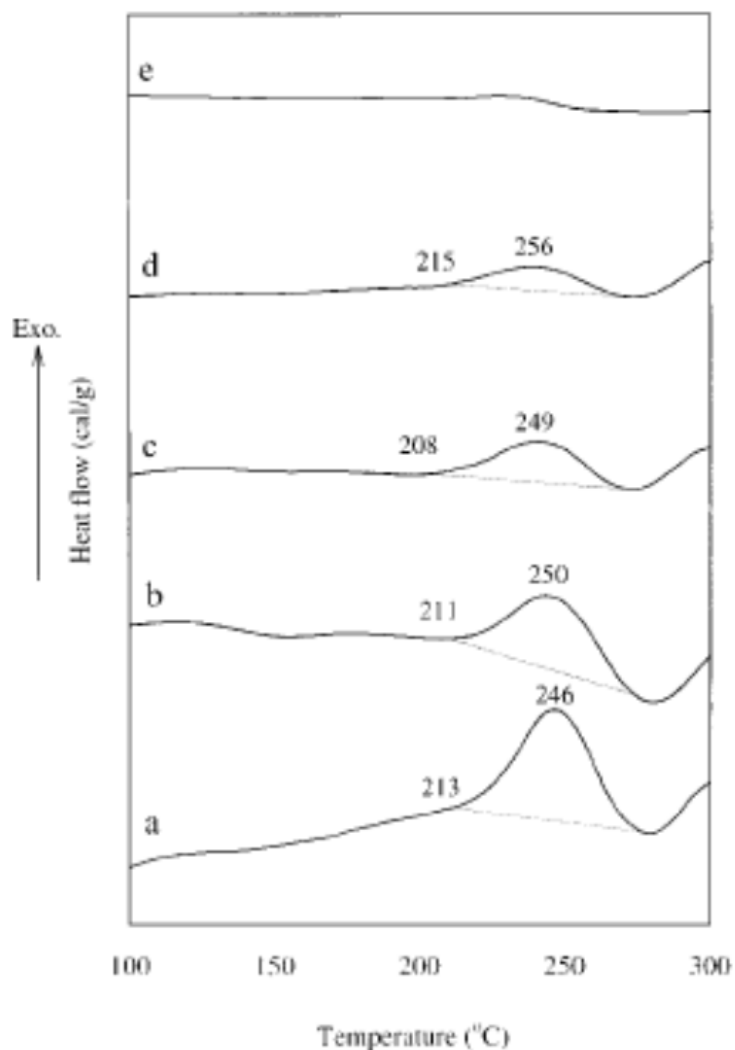


Figure 3.9 DSC thermograms of PU/BA-a (90/10) film treated at various temperatures: (a) 100 °C/1 h, (b) 150 °C/1 h, (c) 170 °C/1 h, (d) 190 °C/1 h and (e) 200 °C/1 h[7].

Thermal stability of the PU/BA-a was also investigated by thermogravimetric analysis (TGA). Figure 3.10 shows TGA profile of the PU/BA-a films. The results revealed that initial decomposition temperatures (5% weight loss) of PU/BA-a films are higher than that of the PU itself and increasing BA-a contents resulted in a higher decomposition temperature. Thus, incorporating polybenzoxazine into PU can open an effective way to an improvement on the thermal stability of the PU.

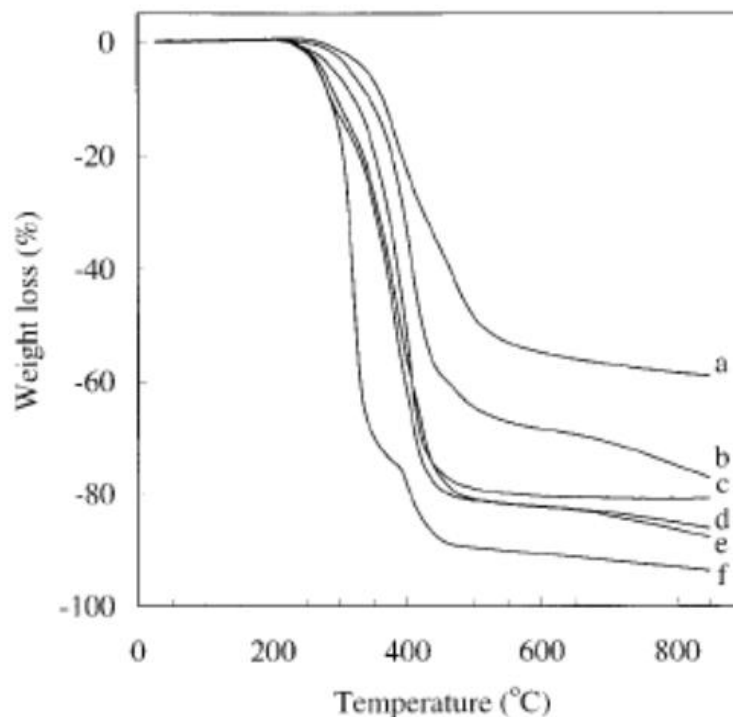


Figure 3.10 TGA analysis of PU/BA-a films: (a) PU/BA-a (0/100), (b) PU/BA-a (70/30), (c) PU/BA-a (80/20), (d) PU/BA-a (85/15), (e) PU/BA-a (90/10), (f) PU/BA-a(100/0)[7].

Lin, M.S. and Chiu, G.A. (1996) [35] investigated curing behavior and mechanical properties of fully and semi-interpenetrating polymer networks based on polyurethane and acrylics. The fully cure IPNs were prepared from polyurethane and poly(ethylene glycol) diacrylate (PEGDA). The DSC thermogram in Figure 3.11 revealed the curing behaviors of these fully and semi IPNs. During the formation of fully IPNs, comparing with PU, all of the exothermic peaks of the fully IPNs shifted to higher value and broader temperature range. The authors concluded that the chain entanglement of the two networks not only provides an additional steric hindrance for the curing reaction but also restrains the chain mobility of the PU and the PEGDA. An increase in temperature would overcome this network interlock effect, thus, shifting the curing exothermic peak to a higher temperature.

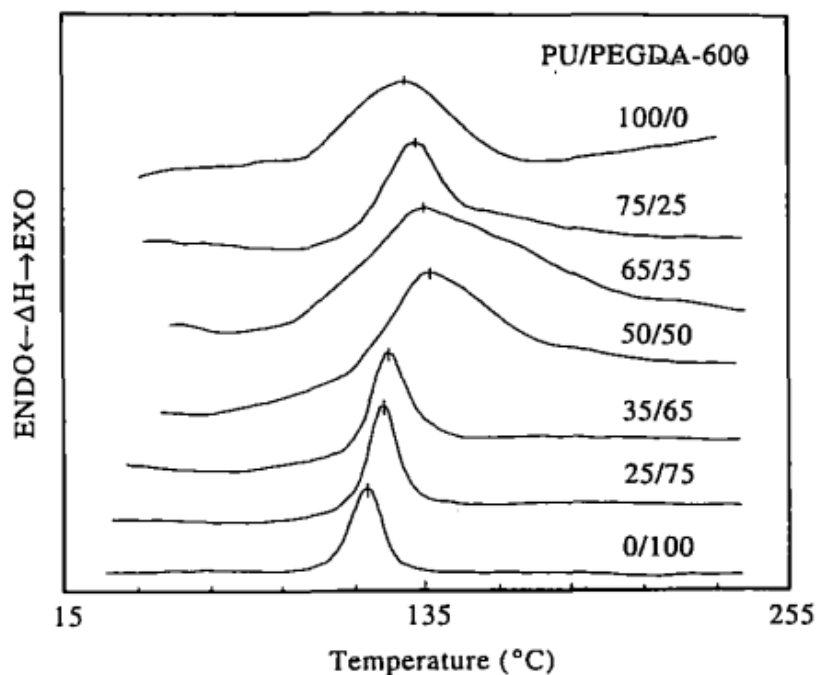


Figure 3.11 DSC thermograms showing the curing exothermic peaks for the fully IPNs based on PU and PEGDA[35].

Lu, C.H., Su, Y.C., Wang, C.F., Huang, C.F., Sheen, Y.C. and Chang, F.C. (2008) [36] studied thermal properties and surface energy characteristics of interpenetrating polyacrylate and polybenzoxazine networks. The UV curing polyacrylate (PA) and the thermal curing polybenzoxazine (PBZ) were prepared separately as solutions in THF and were blended at various mass ratios. Three step procedures were used to prepare the PA/PBZ IPNs: (i) drying in convection oven (ii) photo polymerization (iii) thermal polymerization in convection oven.

Glass transition temperature of the IPNs is shown in Figure 3.12. The thermal properties PBZ polymerization was reported to be suppressed by thermal motion of PBZ, resulting in glass transition temperatures similar to those in the PA/PBZ f-IPNs. The increase in the value of T_g by 10°C was attributed to the steric hindrance of the PA network.

The surface free energies as a function of benzoxazine content of the PA/PBZ IPN are shown in Figure 3.13. In general, low energy additives can migrate to a solid surface to drastically lower its surface tension. The authors, however, found that the PBZ micro-domains were well dispersed in the PA medium likely as a result of $[\text{OH}\cdots\text{O}=\text{C}]$ hydrogen bonds between the two resins. In comparison with the 100% BA-m, the surface free energies of the 40% BA-m in PA/PBZ IPNs increased slightly by 2.6-27.4 mJ/cm^2 .

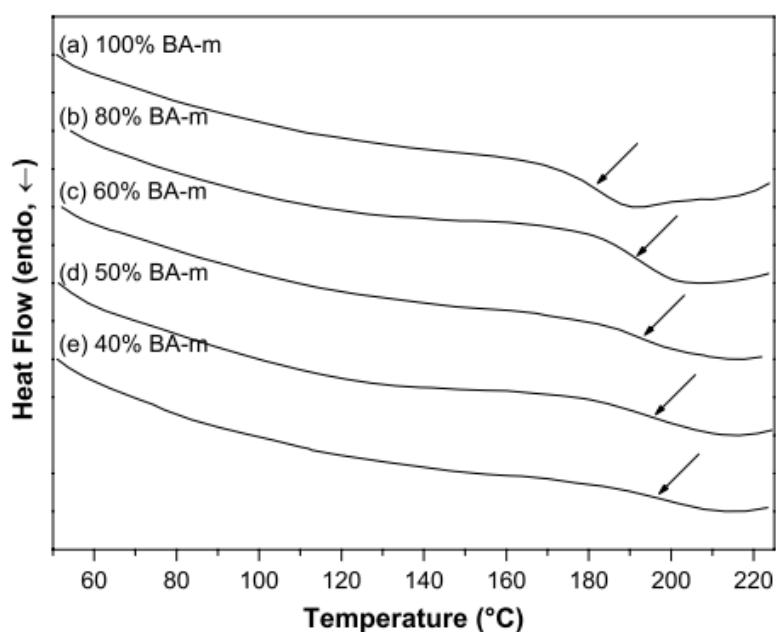


Figure 3.12 DSC thermograms of PA/PBZ IPNs at (a) 100%, (b) 80%, (c) 60%, (d) 50% and (e) 40% of benzoxazine resin (BA-m) [36].

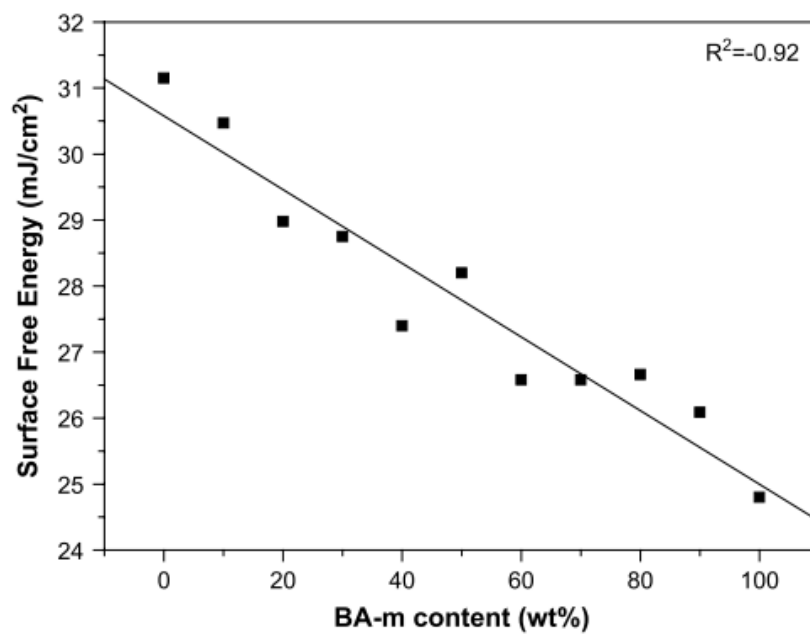


Figure 3.13 Linear relationships between the surface free energies and the BA-m content of the PA/PBZ IPNs [36].

CHAPTER IV

EXPERIMENTAL

4.1 Raw Materials

Raw materials used in this research are bisphenol-A benzoxazine resin, and urethane acrylate prepolymer. Bisphenol-A (polycarbonate grade) was supplied by Thai Polycarbonate Co., Ltd. (TPCC), Thailand. Para-formaldehyde (AR grade) was purchased from Merck Co. while aniline (AR grade) was from PanreacQuimica S.A. Co. The urethane acrylate prepolymer was kindly supplied by CPAC RoofTile Co., Ltd. (Thailand).

4.2 Synthesis of Benzoxazine Monomers

Benzoxazine resin (BA-a) was synthesized from bisphenol-A, para-formaldehyde, and aniline at a molar ratio of 1:4:2. The mixture was heated to 110°C in an aluminum pan and was mixed rigorously for about 30 minutes to yield a light yellow solid monomer product, according to the patented solventless method [23]. The product was then ground into fine powder and can be kept in a refrigerator for a future-use.

4.3 Preparation of Urethane Acrylate-Benzoxazine Polymer Alloys

Urethane acrylate prepolymer (PUA) was blended with benzoxazine resin (BA-a) at various mass ratios, i.e. 100/0, 90/10, 80/20, 70/30, 60/40, 50/50 and 0/100. The mixtures were heated to about 110°C in an aluminum pan and mixed thoroughly until clear homogeneous resin mixtures were obtained. The molten resin mixture was casted onto glass plates by doctor blade for PUA/BA-a film formation. To achieve the fully cured alloy films, firstly, the alloys were cured by ultraviolet light for polymerization of urethane acrylate prepolymer portion followed by thermal curing for ring-opening polymerization of benzoxazine resin in an air-circulated oven. The heat

treatment program for heat curing of the benzoxazine fraction was at 130°C for 1 hr, 150°C for 1 hr, 170°C for 1 hr, 190°C for 1 hr and 200°C for 4 hr. All the specimens were finally left to cool down to room temperature and were then ready for sample characterizations

4.4 Sample Characterizations

4.4.1 Fourier Transform Infrared Spectroscopy (FTIR)

Chemical structure and network formation of a sample was studied by Fourier transform infrared spectroscopy (FTIR). Fourier transform infrared spectra of all samples were acquired by a Spectrum GX FT-IR spectrometer from Perkin Elmer with an ATR accessory. All spectra were taken as a function of time with 512 scans at a resolution of 4 cm^{-1} and a spectral range of 4000-650 cm^{-1} .

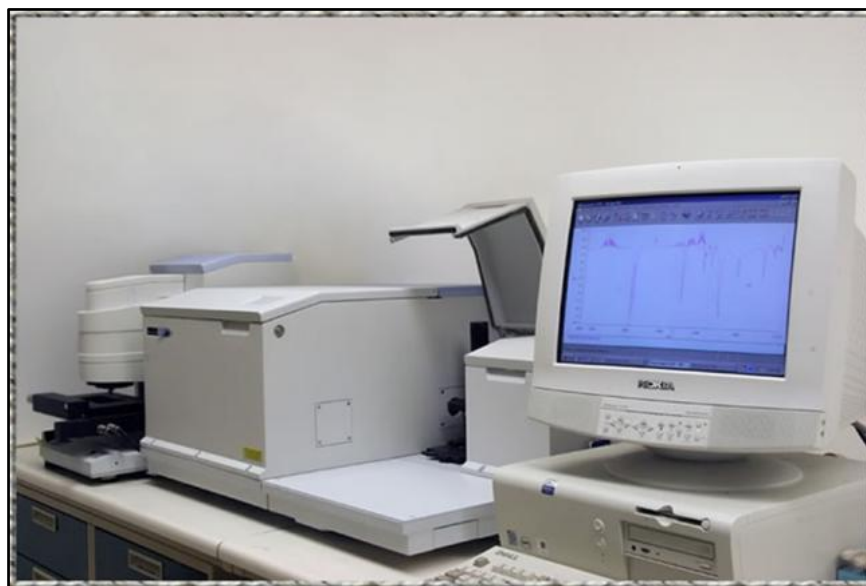


Figure 4.1 Fourier Transform Infrared Spectroscopy (FT-IR) [37].

4.4.2 Differential Scanning Calorimetry (DSC)

A differential scanning calorimeter (DSC) model 2910 from TA Instruments was used to study the curing behaviors of the PUA/BA-a alloys. All samples were put

in aluminum pans with lids. The sample with a mass in a range of 5-10 mg was sealed in an aluminum pan. The DSC thermogram was obtained using a heating rate of 10°C/min from temperature at 30°C to 300°C under a constant flow of nitrogen of 50 ml/min.



Figure 4.2 Differential Scanning Calorimeter (DSC).

4.4.3 Dynamic Mechanical Analysis (DMA)

A dynamic mechanical analyzer (DMA) model DMA242 from NETZSCH was used to investigate the dynamic mechanical properties and relaxation behaviors of PUA/BA-a film alloys obtained from two processing method. The PUA/BA-a film was performed in a tension mode. The temperature was scanned from 30°C to the temperature beyond the glass transition temperatures (T_g) of each specimen with a heating rate of 2°C /min under nitrogen atmosphere. The glass transition temperature was taken as the maximum point on $\tan \delta$ curves.



Figure 4.3 Dynamic Mechanical Analyzer (DMA).

4.4.4 Thermogravimetric Analysis (TGA)

Degradation temperature (T_d) and char yield of the urethane acrylate-benzoxazine polymer alloys at various mass fractions of polybenzoxazine were studied using a thermogravimetric analyzer (TGA) from Perkin Elmer Instrument Technology SII Diamond TG/DTA. The testing temperature program was ramped at a heating rate of $20^\circ\text{C}/\text{min}$ from room temperature to 900°C under nitrogen purging at $100\text{ ml}/\text{min}$. Weight loss of the samples was measured and recorded as function of temperature. The degradation temperature (T_d) of PUA/BA-a alloys was reported at their 10% weight loss. Moreover, the char yields of all samples were also reported at 800°C .

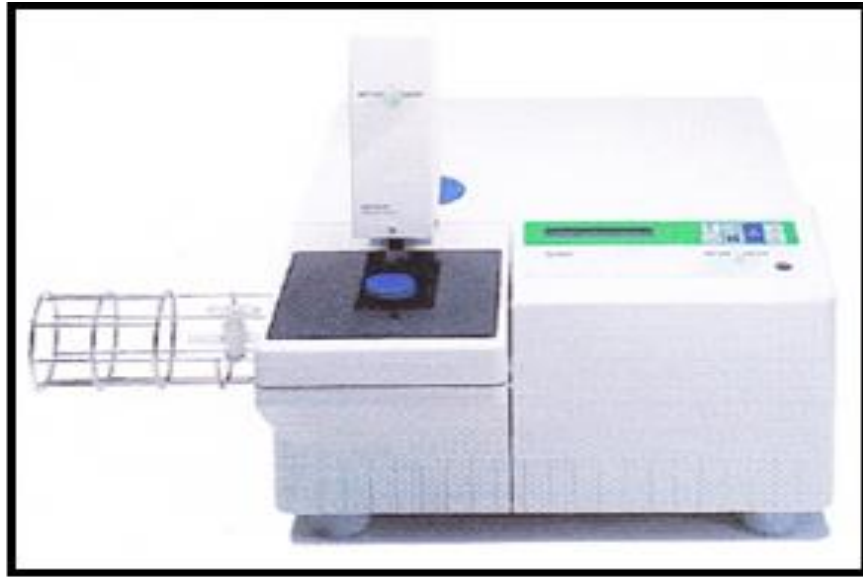


Figure 4.4 Thermogravimetric Analyzer (TGA) [38]

4.4.5 Micro-hardness Tester

Micro-hardness of each polymer alloy was measured utilizing a Vickers micro-hardness tester (model FM-700) from Future-Tech. A pyramidal diamond was applied to the surface of the alloys under a load of 1 kg within 15 s. Diagonal length of the indentation was measured through a micrometric eyepiece with an objective lens (50× magnification). Each sample was measured repeatedly for ten times. The average hardness value of the specimen was calculated by a following equation [29]:

$$HV = 1.854 \frac{L}{d^2} \quad (4.1)$$

Where HV = Vickerhardness value (kg/m²)
 L = Load (kg)
 d = Arithmetic mean of the two diagonals (m)



Figure 4.5 Micro-hardness tester model FM-700[39].

4.4.6 Contact Angle Measurement

Contact angles of the PUA/BA-a alloys at various BA-a composition were studied using a contact angle meter (model 2500702) from Pennyful (Thailand) Co., Ltd. The measurement was to place a water droplet of defined volume on the PUA/BA-a alloy surface, which was always exactly horizontal. To apply reproducible uniform volume drops of de-ionized water, a calibrated micropipette was used. In general, the volume of the water droplet used here was in the range of 25 μl . Drop shape was recorded with a high speed framing camera. Images were then processed by a computer and stored. The droplet shape is then automatically evaluated in terms of contact angle as represented by the angle between the substrate surface and a tangent from the edge to the contour of the drop.



Figure 4.6 Contact Angle Analyzer[40].

4.4.7 Water Absorption Measurement

Water absorption measurement was performed using a specimen dimension of $10 \times 30 \times 0.2 \text{ mm}^3$. Three samples of each composition were submerged in de-ionized water. The specimens were periodically removed and dried by wiping for weight measurements after which they were immediately returned to the water bath. The amount of absorbed water was calculated as the difference between the mass at each of this measurement and the initial conditioned mass. The water absorption was calculated by the following equation:

$$\% \text{ water absorption} = \left(\frac{\text{wet weight} - \text{dried weight}}{\text{dried weight}} \right) \times 100 \quad (4.2)$$

where

wet weight = weight of specimen after water immersion at various time
 dried weight = weight of dry specimen before water immersion at a certain period of time.

4.4.8 Water Vapor Transmission Rate (WVTR)

Water permeation rate of PUA/BA-a alloy films was determined using a water vapor permeability analyzer (MOCON, Permatran-w398, USA), according to ASTM F1249. Each PUA/ BA-a alloy film has a dimension of 5 cm² in area and 0.2 mm in thickness. The WVTR test was carried out at 100% relative humidity and 38°C. The water vapor transmission rate was calculated by the following equation:

$$\text{WVTR} = \frac{\text{mass H}_2\text{O lost}}{\text{time} \times \text{area}} = \frac{\text{flux}}{\text{area}} \quad (4.3)$$

with a unit of g d⁻¹ m⁻². The standard derivation of the WVTR was less than 5%. The WVTR is related to a material characteristic, the water vapor permeability, p , as

$$\text{Permeability} = \text{WVTR} \left(\frac{l}{\Delta p} \right) \quad (4.4)$$

Where l is the film thickness and Δp is the pressure difference across the film. Because the thickness of the film varied, The WVTR was sometime normalized to film thickness (l) to obtain the specific water vapor transmission rate:

$$\text{Permeation rate} = \text{WVTR} \times (l) \quad (4.5)$$

With units of g mil d⁻¹ m⁻¹ [59].



Figure 4.7 Water Vapor Transmission Rater Analyzer (WVTR).

CHAPTER V

RESULTS AND DISCUSSION

5.1 Network Formation of Urethane Acrylate and Benzoxazine Resin Mixture by Fourier Transform Infrared Spectroscopy

The chemical structures of benzoxazine resin, urethane acrylate resin and their network formation reactions were studied by Fourier transform infrared spectroscopy (FTIR). The FT-IR spectra of benzoxazine resin (BA-a) and the fully cured polybenzoxazine are shown in Figure 5.1. Characteristic absorption bands of the BA-a monomer was found at 1229 cm^{-1} assigned to C-O-C stretching mode of benzoxazine ring and 1493 and 942 cm^{-1} assigned to tri-substituted benzene ring. According to the ring-opening polymerization mechanism proposed by Dunkers and Ishida [41], the oxazine ring is opened by the breakage of a C-O bond where the benzoxazine molecule was transformed from a ring structure to a network structure. During this process, the tri-substituted benzene ring and the backbone of the benzoxazine ring became tetra-substituted structure. The ring-opening polymerization of BA-a was observed from a decrease of the absorption band at 1493 and 942 cm^{-1} and the appearance of new adsorption band at 1473 and 875 cm^{-1} which were tetra-substituted benzene ring and the formation of a broad peak at about 3397 cm^{-1} which was assigned to the hydrogen bonding of the phenolic hydroxyl group formation as shown in Figure 5.1b. All important characteristic infrared absorptions of benzoxazine resin and polybenzoxazine structure were clearly observed as described above.

In Figure 5.2a, major characteristic absorption bands of the urethane acrylate prepolymer were identified such as at 1636 cm^{-1} (C=C stretching) and 810 cm^{-1} (C-H stretching) assigned to acrylate double bond. The other characteristic peaks of the resin were at 3375 cm^{-1} from N-H group, at 2940 - 2860 cm^{-1} from aliphatic -C-H stretching, the band at 1720 cm^{-1} from non-H-bonded C=O and the 1686 cm^{-1} resulting from H-bonded C=O. The band at 1520 cm^{-1} was also used to verify the formation of

the NHCOO stretching group. The urethane acrylate prepolymer could produce a crosslink network by reacting with UV light, in our case, at the fixed wavelength of 360 nm (Tokiwa, UVA). Figure 5.2b exhibits FTIR spectrum of polyurethane acrylate after UV curing. The characteristic absorption bands of the acrylate double bond at 1636 cm^{-1} and 810 cm^{-1} clearly disappeared after exposure to the UV light. The behavior implied that the vinyl polymerization reaction had successfully occurred. These observations suggested that urethane acrylate prepolymer had been completely converted to polyurethane acrylate. The gel content of the obtained urethane network at this stage was determined to be 97.4%. The UV cured polyurethane was then heat treated using a step curing at 130°C , 150°C , 170°C , 190°C for 1 hr each, and at 200°C for 4 hr. The resulting FTIR spectrum of the PUA film is shown in Figure 5.2c. From the figure, no significant change in the FTIR spectrum from the UV-cured PUA film was observed from the above heat treatment implying a relatively thermally stable polyurethane network formed after the UV curing. The heat treatment program is the curing condition of benzoxazine resin in this work and this observation also implies no observable chemical change in the urethane network formed by this heat cure program.

The hybrid polymer network between benzoxazine and urethane resins has been reported to show interesting and unique characteristics particularly the observed synergism in its glass transition temperature [42, 43]. Traditional heat curing of benzoxazine and urethane alloys, however, tends to provide a phase separated, opaque, copolymer film and yields a polymer hybrid with rather poor film forming behaviors i.e. non-uniform film thickness. In this work, the hybrid network formation between benzoxazine resin (BA-a) and urethane acrylate prepolymer (PUA) by UV cure followed by thermal cure were examined. Figure 5.3a illustrates FT-IR spectrum of PUA/BA-a resin mixture at 50/50 weight ratio showing mixed characteristic IR bands of both resins as described earlier. The FT-IR spectrum after UV treatment at room temperature depicted in Figure 5.3b clearly revealed the disappearance of the acrylate double bond at 1636 cm^{-1} and 810 cm^{-1} . Moreover, it was observed that the UV cure method merely completed the urethane network formation but did not influence the network formation of the benzoxazine monomers as the characteristic

absorption bands of benzoxazine resin were not altered by UV curing step. For example, the bands at about 1494 cm^{-1} and 946 cm^{-1} of the tri-substituted benzene ring in benzoxazine monomers were remained in this spectrum. However, after thermal cure, these absorption peaks of the tri-substituted benzene ring and the backbone of the benzoxazine ring became tetra-substituted causing the disappearance of these bands as seen in Figure 5.3c. In summary, the curing of benzoxazine and urethane resins in our work can be achieved by sequential cure method consisting of (i) UV cure for polyurethane acrylate network formation and followed by (ii) thermal cure for polymerization of the benzoxazine fraction. The proposed sequential cure of the resin mixture provided the hybrid film of highly uniform thickness with fast film forming characteristic of the urethane acrylate fraction. It is also highly likely that the hybrid network formed is of an interpenetrating polymer networks, IPNs, type as both resins experience totally different curing mechanisms and cured separately as discussed above. To confirm this postulation, other major properties of the polymer hybrid were also evaluated.

5.2 Determination of Fully Cured Condition of PUA/BA-a Alloy Films by Differential Scanning Calorimetry

Figure 5.4 presents an effect of the heat treatment on curing exotherms of PUA/BA-a resin mixture at 50/50 mass ratio. From the thermograms, the curing exothermic peak of the resin mixture was observed at 246°C . This peak temperature is assigned to the curing peak of the thermally curable benzoxazine fraction in the mixture which shows the curing peak temperature of 232°C . It is evident that the presence of the PUA fraction causes a shift of the exothermic curing peak of the benzoxazine resin to higher temperature. In our previous work, the same phenomenon in the resin mixtures of elastomeric PU resin with BA-a under thermal curing was also reported [44]. The behavior was attributed to the dilution effect of the PU fraction on the BA-a curing reaction. After heat treatment at elevated temperature, the area under the exothermic peaks expectedly decreased with increasing curing temperature. The peak position was also found to further shift slightly to higher temperature. This phenomenon was due to the increase in curing conversion of the benzoxazine resin

with the temperature to form a benzoxazine gel or network which can further restrict the mobility of the residual monomers. The curing retardation was thus observed. After the heat treatment at 200°C for 4 hours, the exothermic peak was found to completely disappear indicating the fully cured stage of the resin mixture. The same heat treatment program was also used to obtain fully cured polybenzoxazine hybrids of the same kind [42-44].

5.3 Characterizations of the PUA/BA-a Alloy Films

5.3.1 Dynamic Mechanical Analysis of the PUA/BA-a Alloy Films

Thermomechanical properties of the sequential cured PUA/BA-a alloy films with BA-a mass fraction ranging from 0-50% by weight were investigated by a dynamic mechanical analyzer (DMA). The obtained DMA thermograms are illustrated in Figure 5.5. From this figure, the storage modulus of the solid PUA/BA-a polymer alloys at their glassy state was found to increase with increasing BA-a mass fraction. The storage modulus at room temperature of the neat polyurethane acrylate (PUA) and the polybenzoxazine (PBA-a) were determined to be 1.3 GPa and 2.6 GPa, respectively whereas their alloys showed the storage modulus values of 1.6 GPa in PUA/BA-a 90/10, 2.0 GPa in PUA/BA-a 80/20, 2.1 GPa in PUA/BA-a 70/30, 2.1 GPa in PUA/BA-a 60/40 and about 2.3 GPa in PUA/BA-a 50/50. This result suggests that the PUA is less stiff than the PBA-a due to the presence of soft aliphatic segments in its molecular structure compared to the more prevalent aromatic structure in the PBA-a network. Moreover, modulus-temperature curves at glassy state of the PUA/BA-a alloys showed a decrease in their slopes as the mass fraction of the BA-a increased. This observed characteristic implies enhanced thermal stability of the polymer alloys by the presence of the more thermally stable PBA-a in the PUA network.

Effects of PBA-a on storage modulus in the rubbery plateau region of their PUA/PBA-a alloys are illustrated in Figure 5.5. In contrast to the glassy state modulus, the storage modulus in the rubbery plateau region of the polymer alloys was observed to decrease with mass fraction of the PBA-a. The storage moduli of the

alloys in the rubbery plateau were decreased from 127 MPa to 84 MPa with an addition of the BA-a fraction from 0 to 50% by weight. This result suggests that the increase in the BA-a content in the polymer alloys resulted in a decrease in crosslink density of the fully cured specimens which was closely related to the rubber plateau modulus. Crosslink density of a polymer network can be estimated from the theory of rubber elasticity by knowing its rubbery plateau modulus as suggested by Nielson [45-46].

$$\log\left(\frac{E'}{3}\right) = 6.0 + 293(\rho_x) \quad (5.1)$$

From Nielson's equation above, E' is a storage modulus in a rubbery plateau region, ρ_x is a crosslink density that is the mole number of network chains per unit volume of the polymers. The crosslink density determined from Nielson's equation of PUA/PBA-a alloys is shown in Figure 5.6. From the results, the crosslink densities of the PUA/BA-a polymer alloys were slightly decreased from 5,554 to 4,931 mol/m³ with an addition of the BA-a fraction from 0 to 50% by weight. Polybenzoxazine is a well-known thermoset that possesses a relatively low crosslink density compared to epoxy, phenolics or polyurethane [42]. Some recent works reported the neat PBA-a to possess a crosslink density value ranging from 4000-4350 mol/m³ [36, 37]. Despite the rather low crosslink densities observed, polybenzoxazines exhibit high glass transition temperatures as a result of their unique intramolecular [O...NH⁺] interactions [36, 47].

Glass transition temperature (T_g) and network characteristics of the PBA-a and the PUA/BA-a alloys were examined from $\tan \delta$ curves of the DMA thermograms exhibited in Figure 5.7. $\tan \delta$ is determined from the ratio of a viscous part (E'') to a storage energy or elastic part (E') of dynamic modulus of material. The peak of the $\tan \delta$ can be used to identify glass transition temperature of a polymer. From the curves in Figure 5.7, the T_g s of the alloys were found to increase as the BA-a content increased i.e. from 124°C of the neat PUA to the value of 129°C, 148°C, 162°C, 180°C and 210°C at the BA-a contents of 10, 20, 30, 40, and 50wt% respectively. Interestingly,

the T_g from $\tan \delta$ of the neat PBA-a was determined to be 188°C and similar synergistic behavior in T_g of the polymer hybrids between polybenzoxazine and polyurethane is also observed in this work. The same synergistic behavior was also reported in thermally cured copolymers of these two families of polymers [42, 43] and was explained as due to the complementary property of the two polymers i.e. the enhancement in crosslink density in the polybenzoxazine fraction by the presence of the PUA and the improvement in network rigidity of the polyurethane by the presence of the more rigid polybenzoxazine [42, 43].

Careful inspection of the $\tan \delta$ curves for each polymer alloy composition reveals only one peak that can be associated with the α relaxation or glass transition. If the two starting materials exhibit phase separation and have prevented copolymerization, then two glass transition peaks for each homopolymer would be expected in the $\tan \delta$ curve. Similar behavior has been observed for immiscible and partially miscible polymer blends. The appearance of only single $\tan \delta$ peak associated with the glass transition in our polymer alloy supports the previous hypothesis that both resins in fact formed a highly compatible hybrid network without detectable phase separation. The visual appearance of the obtained PUA/PBA-a is also illustrated in Figure 5.8. From this figure, all PUA/PBA-a alloy films are relatively transparent with the color ranging from yellow in neat PUA to brown color in PUA/BA-a 50/50 and in the neat PBA-a. This optical property also confirms the highly compatible nature of the two polymers in the obtained hybrids.

The height and width at half height of the $\tan \delta$ peak for each PUA/BA-a alloy films is summarized in Figure 5.9. The shape of $\tan \delta$ peak can be used as a convenient indicator of the morphological state of the phases within the polymer hybrids. The broadness of a relaxation indicates the complexity of the network structure. Although only one $\tan \delta$ peak was observed for these PUA/BA-a alloy systems, their $\tan \delta$ peaks tend to become broader with increasing BA-a content, which is indicated by an increase in width at half height of $\tan \delta$ peaks. The maximum width at half height of our PUA/BA-a alloys was observed at the BA-a content of 50% by weight, the composition which maintains UV curability of the alloy films. An

addition of BA-a to 60% by weight resulted in a narrower width at half height as seen in Figure 5.9. This behavior is consistent with the fully interpenetrating polymer network based on polyurethane and acrylics investigated by Lin and Chiu [36]. In this report, the authors suggested that the fully IPN's possess broader width at half height than semi-IPN's. The maximum width at half height of the $\tan \delta$ was reported to occur at the resin mixture composition of 50/50 as this composition contains the largest extent of network interlock. In practice, the wider the width at half of the $\tan \delta$, the better the cracking energy is absorbed by the material [35]. Beyond 50% by weight of the BA-a, the width of damping $\tan \delta$ peak became less broadened suggesting lessened network interlock and the material is expected to absorb less cracking energy thus tends to provide lower impact resistance. In addition, it is evident that the widths at half of the $\tan \delta$ of the PUA/BA-a alloys are broader than those of the neat PUA and polybenzoxazine and our results are in good agreement with the Polyurethane and Acrylics IPNs systems [35].

From the view of molecular structures, the height of the $\tan \delta$ peak reflects the viscous nature of a material. The higher the $\tan \delta$, the more viscous or fluid-like the material is. In Figure 5.9, it can be seen that the height of $\tan \delta$ peaks of BA-a polymer alloys decreased with increasing BA-a concentration in the range of 0-60% by weight. This behavior is caused by the presence of the more bulky and rigid benzoxazine network that can substantially restrain the segmental mobility and lower relaxing species of the hybrid networks. This result is also in accordance with the systematic enhancement in the glassy state modulus of the polymer alloys with the amount of the PBA-a discussed previously. The restriction of chain mobility of the PUA network by the PBA-a network was further evaluated from the determination of activation energy of the α relaxation or glass transition of each polymer alloys.

5.3.1.1 Analysis of Activation Energy (ΔE_a) of Glass Transition Temperature of the PUA/BA-a Alloy Films

Multi-frequency dynamic mechanical analysis has been demonstrated by many workers to be a powerful tool for the determination of activation energy of major and

minor transitions or relaxations as well as to follow crystallization and structural changes in polymers [48-55]. This technique is used to quantify apparent activation energy of the glass transition temperature of the PUA/BA-a alloys as a function of their compositions in order to observe their effect on the chain mobility of the resulting hybrid networks.

Figure 5.10 shows the variation of T_g obtained from $\tan \delta$ peak as a function of frequency of the dynamic mechanical spectra of PUA/BA-a 50/50 alloy films. With increasing test frequency, the storage modulus and the $\tan \delta$ curves were found to shift to higher temperature. The Arrhenius plot between the peak temperatures of the loss tangent and the frequencies of the glass transition temperature of PUA/BA-a alloys at varied compositions renders activation energy for this transition. As seen in Figure 5.11, a good linear correlation was observed in the Arrhenius plots, and the activation energy was also calculated from the slope of the relationship between the frequency and glass transition temperature. The obtained activation energy values were summarized in Table A-4. The activation energy of PUA/BA-a polymer alloys tended to increase with increasing amount of BA-a content e.g. 406 kJ/mole (PUA), 424 kJ/mole (PUA/BA-a 90/10), 431 kJ/mole (PUA/BA-a 80/20) up to the value of 481 kJ/mole (PUA/BA-a 50/50). The increase in BA-a content in the alloys up to 50% by weight might increase the degree of network interlock with the PUA network as described previously in the analysis of the $\tan \delta$ curves. This would cause greater restriction in the mobility of the polymer chains in the network, leading to an increase in activation energy of the glass transition above.

5.3.2 Thermal Degradation of the PUA/BA-a Polymer Alloy Films

Thermal stability of PUA/BA-a film alloys under the sequential cure process was investigated by thermogravimetric analysis (TGA) under N_2 atmosphere and the thermograms of the alloys at various BA-a content are shown in Figure 5.12. Thermal stability of PUA/BA-a film alloys were evaluated by comparing their degradation temperature (T_d) at 10% weight loss. From the TGA thermograms, the thermal decomposition in each alloy was found to show mainly a single stage weight loss. The

T_d 's of the neat PBZ and the neat PUA were determined to be 344°C and 368°C whereas their alloys showed the T_d values of 363°C in PUA/BA-a 90/10, 361°C in PUA/BA-a 80/20, 360°C in PUA/BA-a 70/30, 359°C in PUA/BA-a 60/40 and 357°C in PUA/BA-a 50/50 respectively. T_d 's of the polymer alloys were found to slightly decrease in a linear manner with increasing the mass fraction of the BA-a as shown in an inset of Figure 5.12. Additionally, the T_d 's of the obtained alloys were found to be higher than those reported interpenetrating polymer network systems e.g. 301-367°C for blocked PU/epoxy [4], 328-334°C for PBa/EPU [9] and 338-341°C for PU/PA [60]

Furthermore, the char yield of PUA/BA-a alloys under the same sequential cure methods, reported at 800°C under N_2 atmosphere, was illustrated in Figure 5.12. In this figure, the polybenzoxazine had a char yield value of about 33% while the polyurethane acrylate had a char yield value of only 5%. In addition, the residual weight of the PUA/BA-a alloys was found to systematically increase with increasing BA-a mass fraction. The char yield values of PUA/BA-a alloys of 7.6% in PUA/BA-a 90/10, 8.2% in PUA/BA-a 80/20, up to the value of 16.9% in PUA/BA-a 50/50 were obtained, The enhancement in char formation of the PUA/BA-a alloys was found to show a linear relationship with the amount of the polybenzoxazine as clearly seen in an inset of Figure 5.12. In principle, the higher the char yield, the better the fire resistant behavior of the polymer. The improving fire resistant behavior of the alloys as a result of the presence of greater char forming polybenzoxazine fraction is clearly one key benefit from this polymer hybrid.

5.3.3 Hardness Properties of the PUA/BA-a Alloy Films

Local surface hardness of the PUA/BA-a specimens, which is generally investigated as one of the most important factor that relates to wear resistance of a material, was characterized via micro-hardness determination. This measurement is a powerful tool for probing mechanical property of a material in small volume. Figure 5.13 depicts surface hardness (H) at room temperature (25°C) of PUA/BA-a hybrid polymer samples as a function of BA-a content. From the results, we can see that the

hardness of the PUA/BA-a samples steadily increased with increasing the BA-a content. The surface hardness values of the fully cured PUA/BA-a alloys were observed to be 139 MPa in the pure PUA, 152 MPa in PUA/BA-a 90/10, up to the value of 232 MPa in PUA/BA-a 50/50 and 404 MPa in the pure polybenzoxazine. The observed hardness of the PUA/BA-a alloys tended to follow a simple rule of mixture as seen in the same figure. This substantial improvement in hardness of the PUA/BA-a alloy films were attributed to a greater molecular rigidity of the BA-a in the PUAnetwork. This kind of UV curable polyurethane is presently used as a top coat of cement roof tile by The CPAC Roof Tile Co., Ltd, Thailand etc. One key requirement of this kind of product is to provide improved hardness and wear resistance of the top coat material. Consequently, the presence of the BA-a in the alloys helps improve the required hardness and wear resistance of the PUA coating.

5.3.4 Water Absorption Properties of the PUA/BA-a Alloy Films

Figure 5.14 shows percent water absorption of PUA/BA-a film alloys versus time. It can be seen in this figure that the percent water absorption value of PUA alloyed with the BA-a tended to decrease with an addition of the BA-a. Moreover, the percent water absorption was observed to increase sharply in the first 24 hours of the test, and reach a plateau value of 2.0% in the pure PUA, 1.9% in PUA/BA-a 90/10, 1.8% in PUA/BA-a 80/20, and 1.4% in PUA/BA-a 70/30, 1.3% in PUA/BA-a 60/40 and 1.2% in PUA/BA-a 50/50. The reason for this phenomenon was explained as due to the lower number of hydroxyl group from the incorporation of the BA-a fraction and was confirmed by the FT-IR measurement (Figures 5.1 and 5.2). The less the hydroxyl group presented, the lower the polarity of the polymers thus resulting in the decrease in water absorption of the alloys.

5.3.5 Water Contact Angles of the PUA/BA-a Alloy Films

Hydrophobicity is a highly desirable property for materials that are used in a wide range of applications. The distributions of hydrogen bonding, i.e. inter- and intra-molecular H-bonding is an important factor in deciding the contact angle of the

polymer. The contact angle represents the wet ability of a solid surface when liquid forms homeostasis by thermodynamics. Low contact angle displays high wet ability (hydrophilic property) and high surface energy, and high contact angle means low wet ability (hydrophobic property) and low surface energy. Because the contact angle of liquid drop on the flat solid surface is measured at the contact point of solid surface and end point of water droplet curvature, the contact angle between solid surface and liquid is analytical tool of physical and chemical characteristics which is used much in (adhesion), surface treatment or polymer surface analysis. Variations in the surface hydrophobicity of PUA/BA-a alloy films were evaluated by the measurement of contact angles with water. Figure 5.15 shows the water contact angles of PUA/BA-a alloy films. The water contact angle on the unmodified PUA and the neat polybenzoxazine were determined to be 92.9° and 107.7° suggesting the less polarity of the polybenzoxazine compared to the polyurethane. The water contact angles on the PUA/BA-a alloy films expectedly increased with increasing the BA-a content. The water contact angle values of the PUA/BA-a alloy films were observed to be 93.9° in PUA/BA-a 90/10, 94.9° in PUA/BA-a 80/20, 95.5° in PUA/BA-a 70/30, 96.9° in PUA/BA-a 60/40, 100° in PUA/BA-a 50/50, respectively. That is the values were found to be increased with increasing the BA-a contents. This result implies that the presence of the more hydrophobic BA-a improves the water resistant property of the resulting alloy films thus enhances the water repellent property and cleanability of the PUA/BA-a alloy films which it is important properties for roof tile coating materials.

5.3.6 Water Vapor Transmission Rate of the PUA/BA-a Alloy Films

In coating application, high moisture content and fast moisture/gas transmission considerably restrict a material's useful potential [56, 57]. The reduction of moisture transfer can suppress internal damage and improve long-term performance. Therefore, high performance coating films must be able to prevent or at least decrease moisture transfer between the rigid substrate and the surrounding atmosphere i.e. water permeability should be as low as possible. The permeation rates of PUA film, BA-a film and their alloy films are shown in Figure 5.16. The permeation rates of the PUA/BA-a alloy films were determined to be 254 gm-mil/m^2 -

day in the pure PUA, 153 gm-mil/m²-day in PUA/BA-a 90/10, 152 gm-mil/m²-day in PUA/BA-a 80/20, 129 gm-mil/m²-day in PUA/BA-a 70/30, 124 gm-mil/m²-day PUA/BA-a 60/40, 94 gm-mil/m²-day PUA/BA-a 50/50 and only 33 gm-mil/m²-day in the neat polybenzoxazine. Obviously, the permeation rates of the PUA alloyed with BA-a were found to be substantially reduced with the amount of the BA-a. It is well-known that water adsorption and transport behaviors depend on both morphological and chemical structure i.e. chain packing, side group, and polarity [58]. Based on water contact angle, water adsorption, and water permeability results, it is evident that the water resistant capacity of the neat PUA film is greatly enhanced by incorporating the BA-a content thus makes the alloy films highly attractive for coating application.

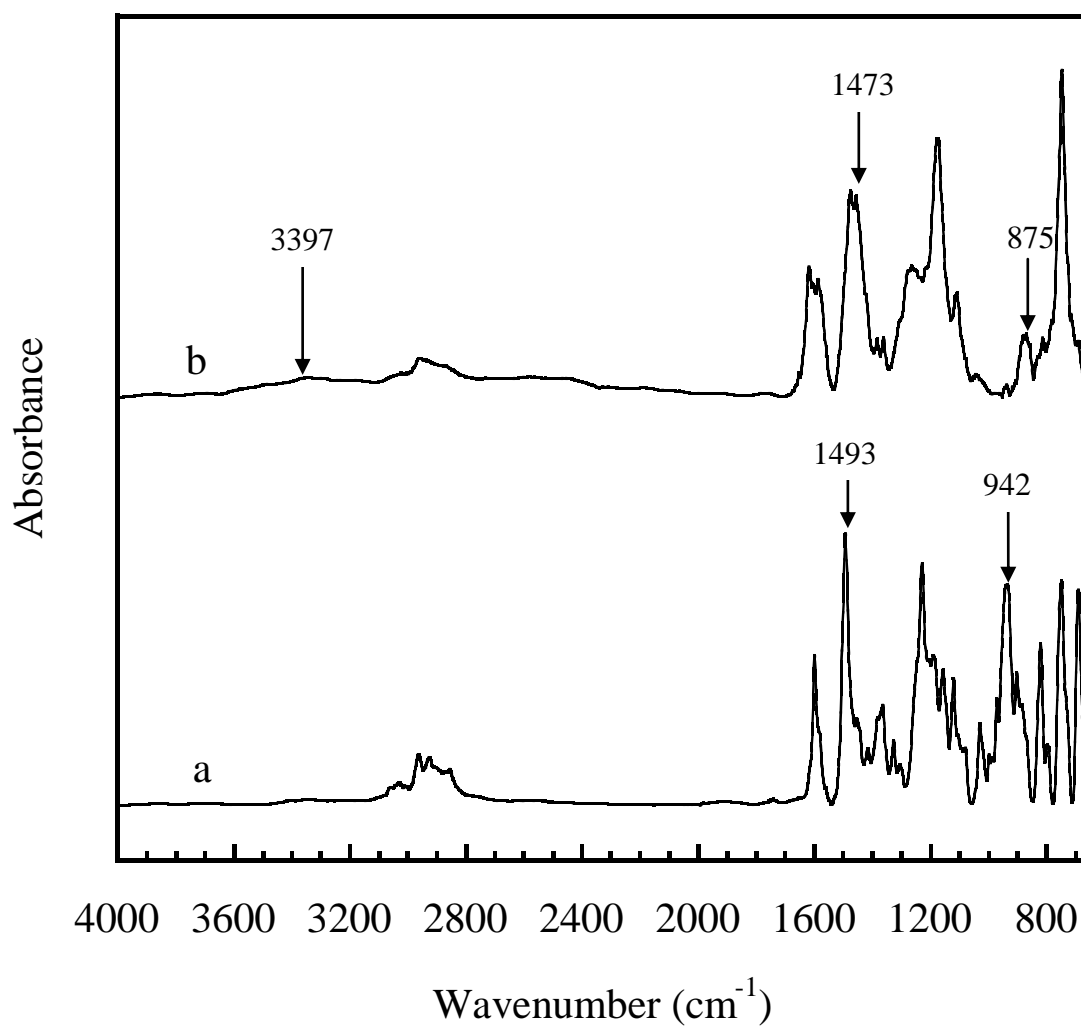


Figure 5.1 FT-IR spectra of benzoxazine resin: (a) BA-a resin (BA-a),
(b) Polybenzoxazine.

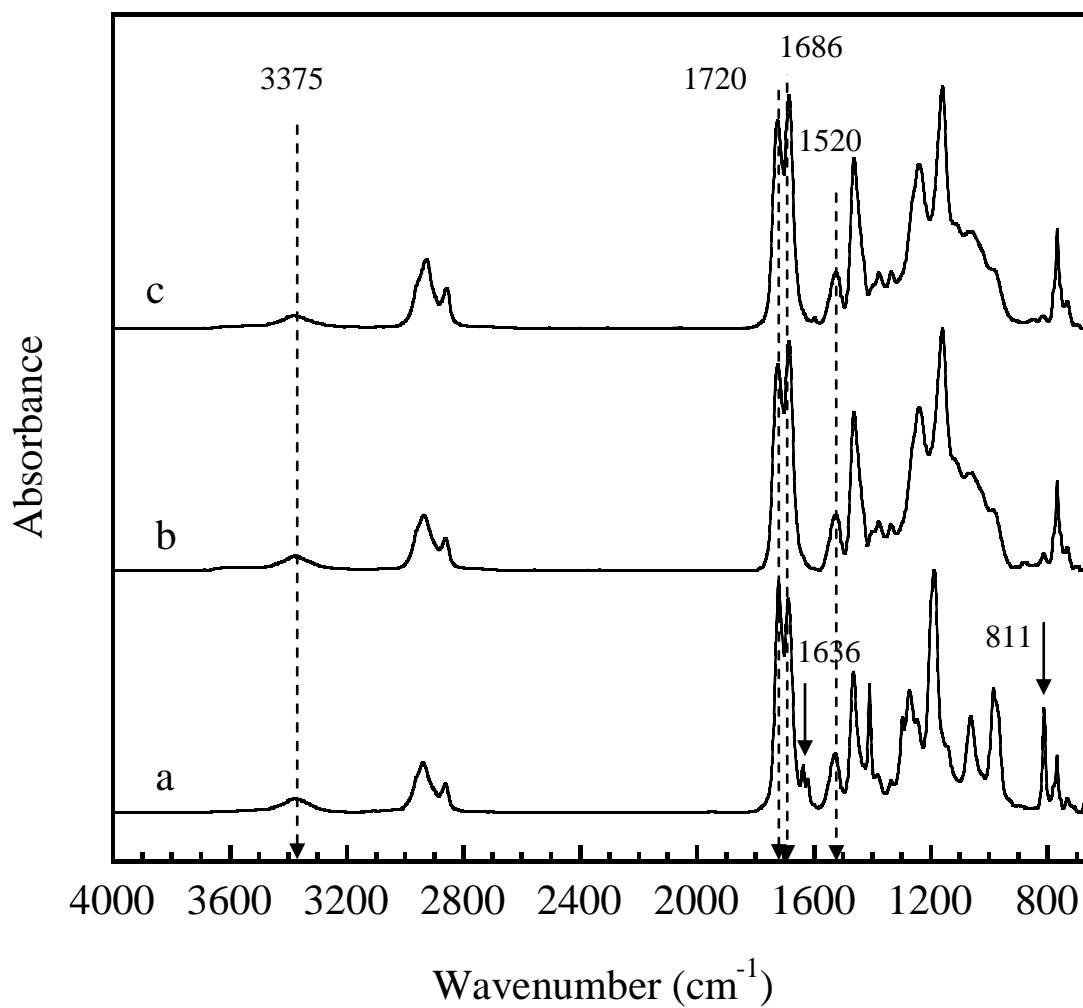


Figure 5.2 FT-IR spectra of urethane acrylate prepolymer: (a) Urethane acrylate Prepolymer (PUA), (b) PUA after UV cure, (c) PUA after UV and thermal cure.

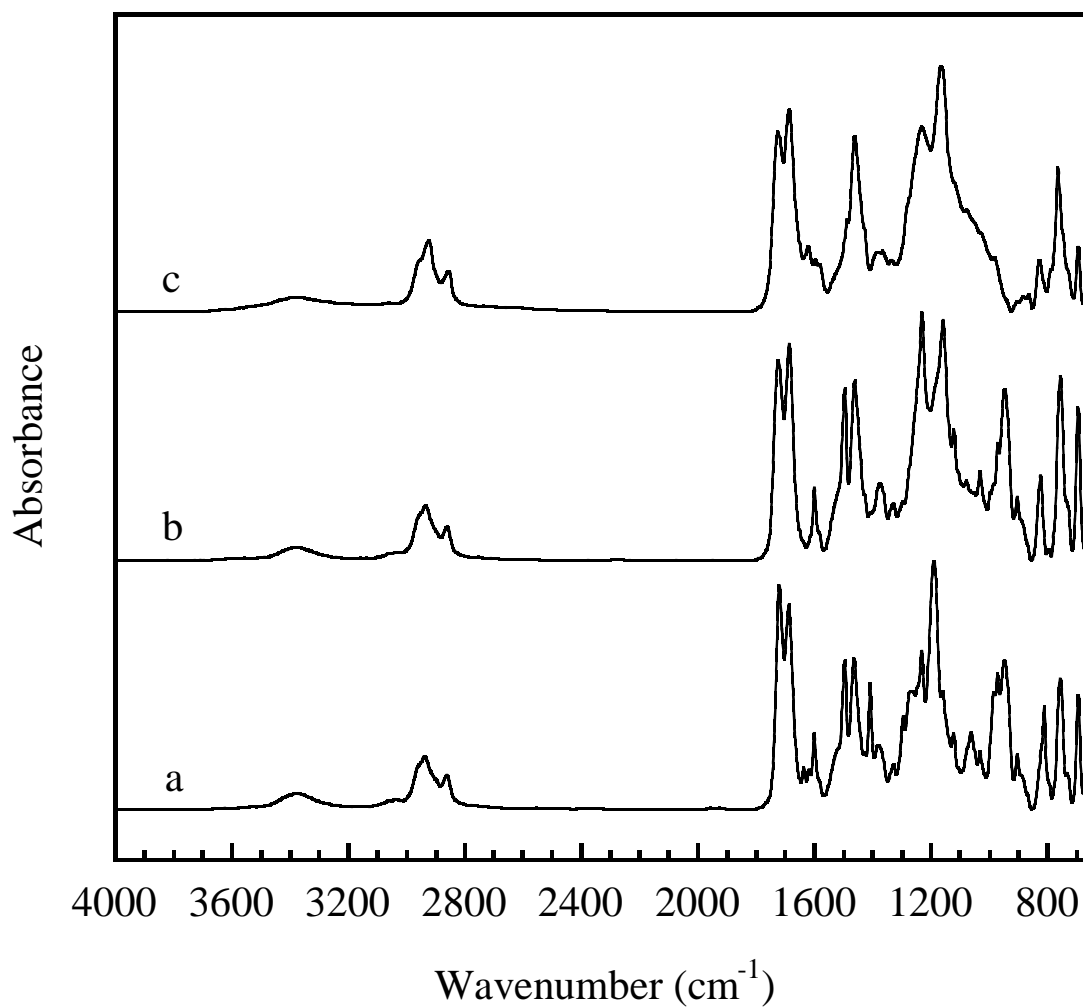


Figure 5.3 FT-IR spectra of PUA/BA-a alloys at 50/50 weight ratio: (a) PUA/BA-a resin mixture (b) PUA/BA-a after UV cure, (c) PUA/BA-a after UV and thermal cure.

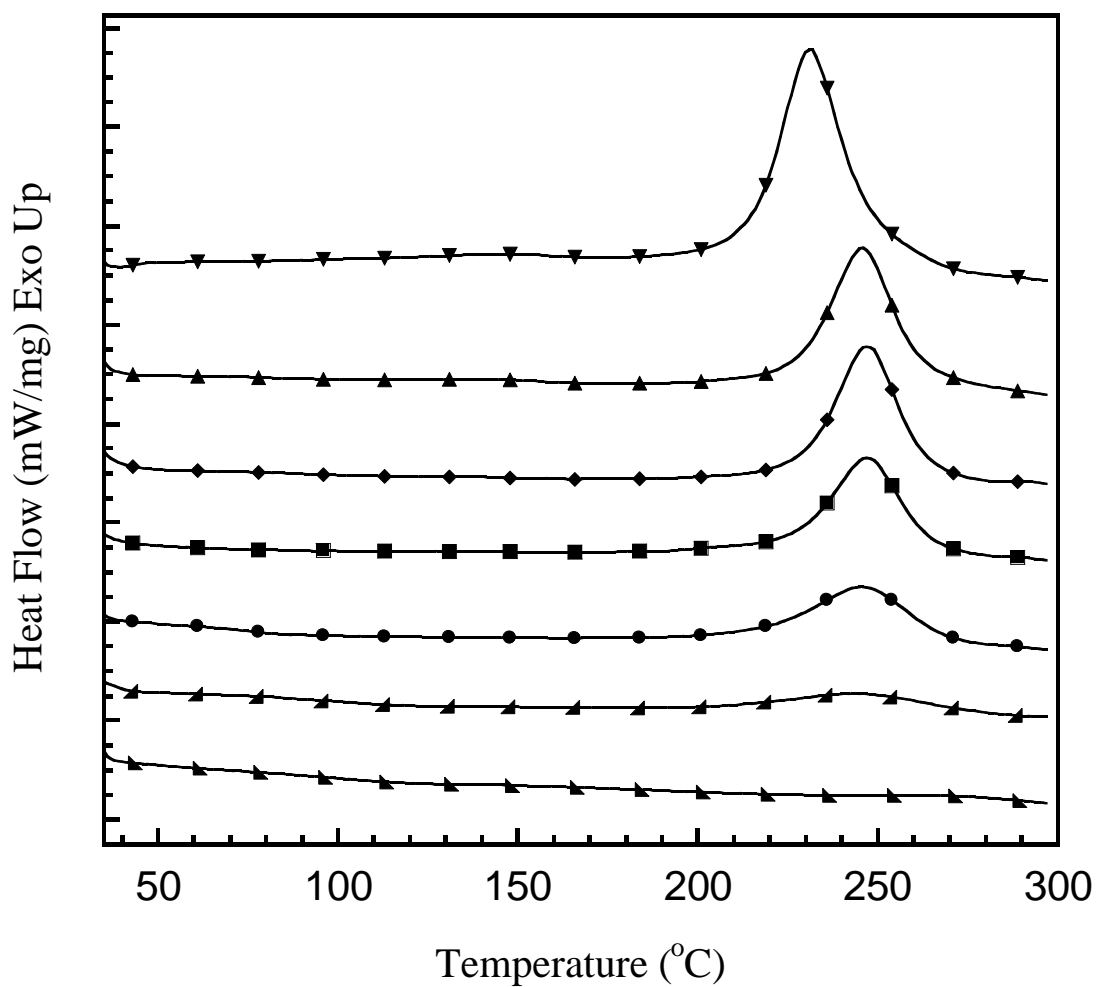


Figure 5.4 DSC thermograms of the PUA mixed with BA-a resin at a mass ratio of 50:50 at various curing conditions: (▼) BA-a monomer, (▲) After UV cure, (◆) 130°C/1hr, (■)150°C/1hr, (●) 170°C/1hr, (◀) 190°C/1hr (▶) 200°C/4hr.

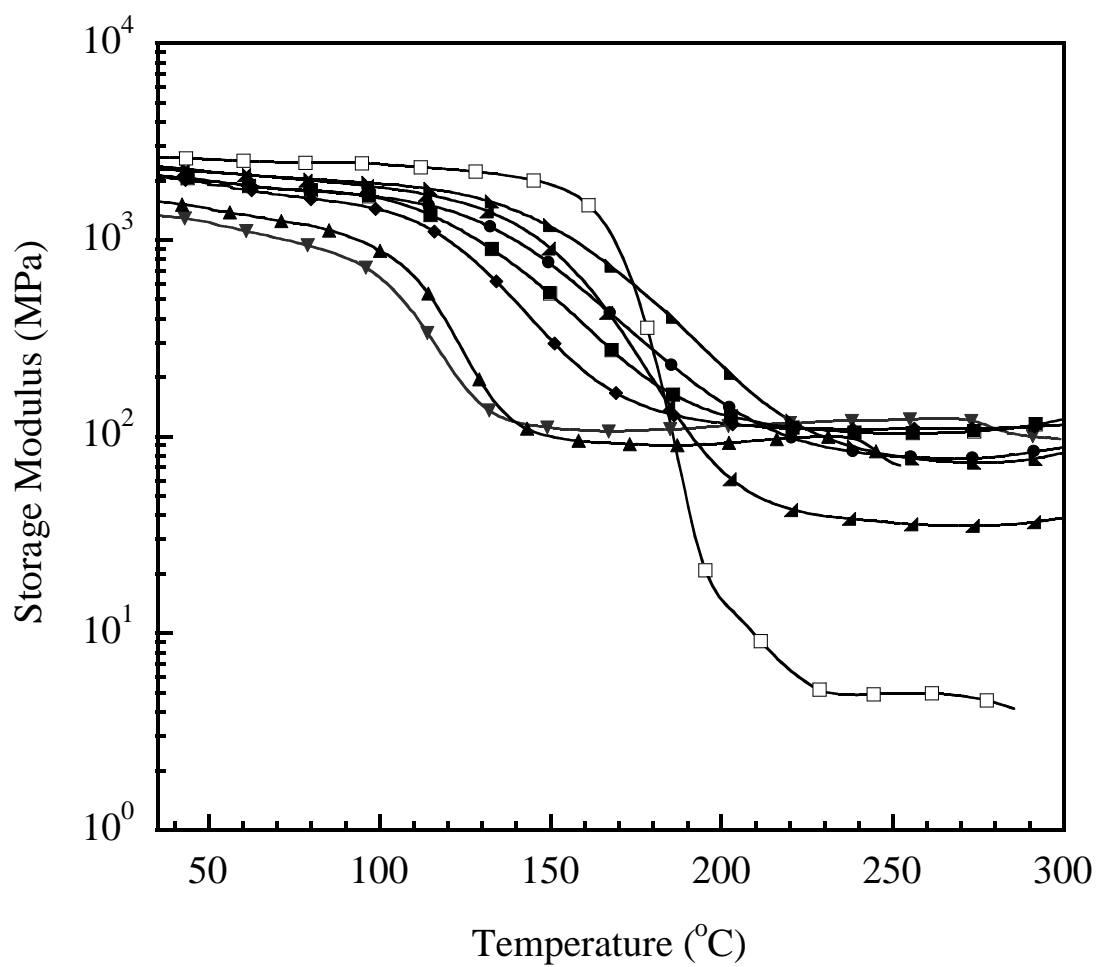


Figure 5.5 Storage modulus of PUA/BA-a alloy films at various compositions:
(▼) 100/0, (▲) 90/10, (◆) 80/20, (■) 70/30, (●) 60/40, (▸) 50/50,
(◀) 40/60, (□) 0/100.

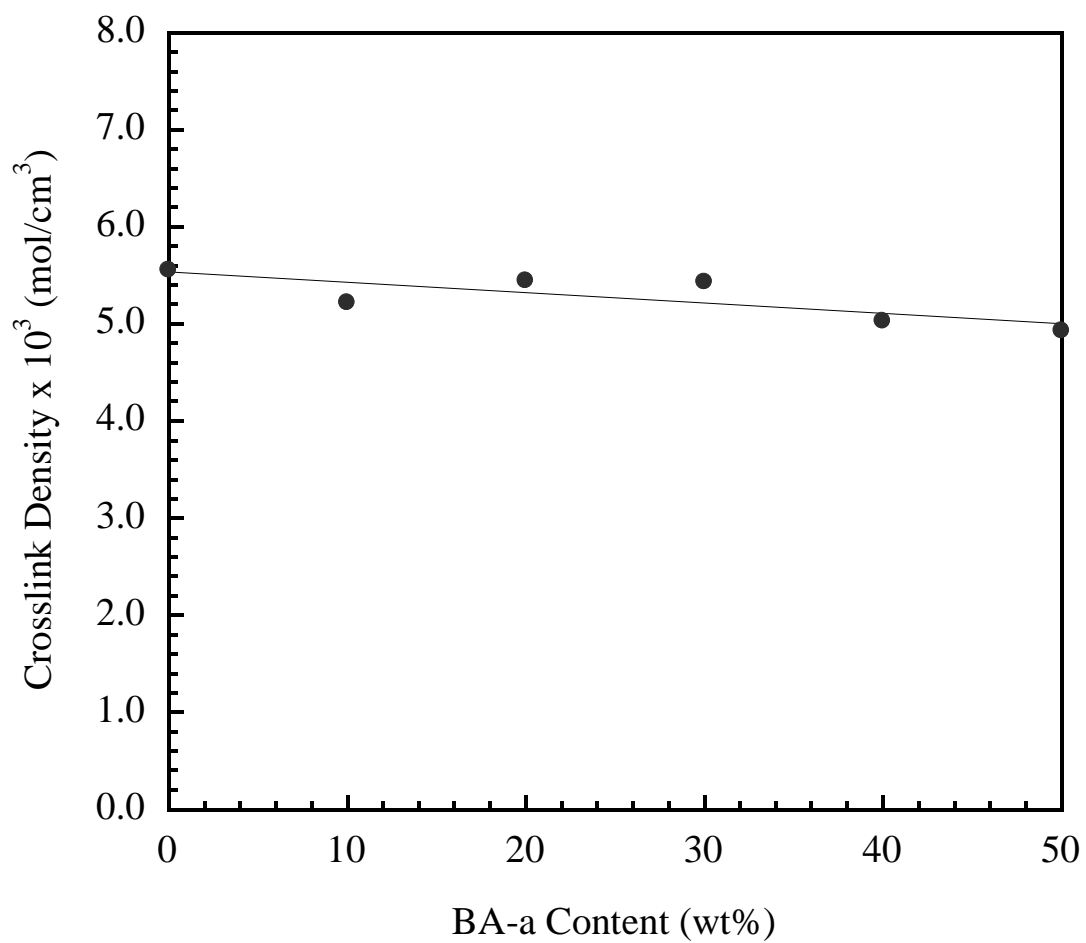


Figure 5.6 Crosslink densities of PUA/BA-a alloy films at various compositions.

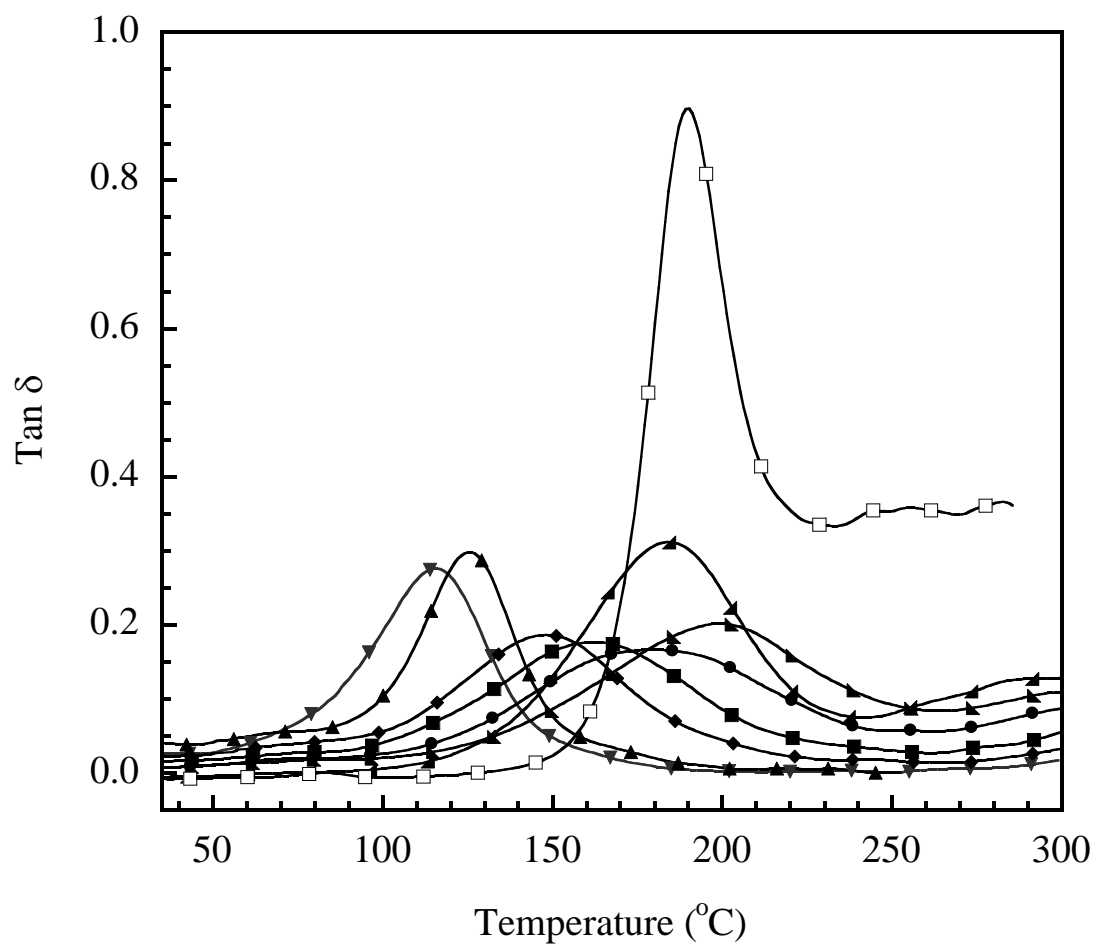


Figure 5.7 Tan δ of PUA/BA-a alloyfilms at various compositions:(▼) 100/0, (▲) 90/10, (◆) 80/20, (■) 70/30, (●) 60/40, (♣) 50/50, (♠) 40/60, (□) 0/100.

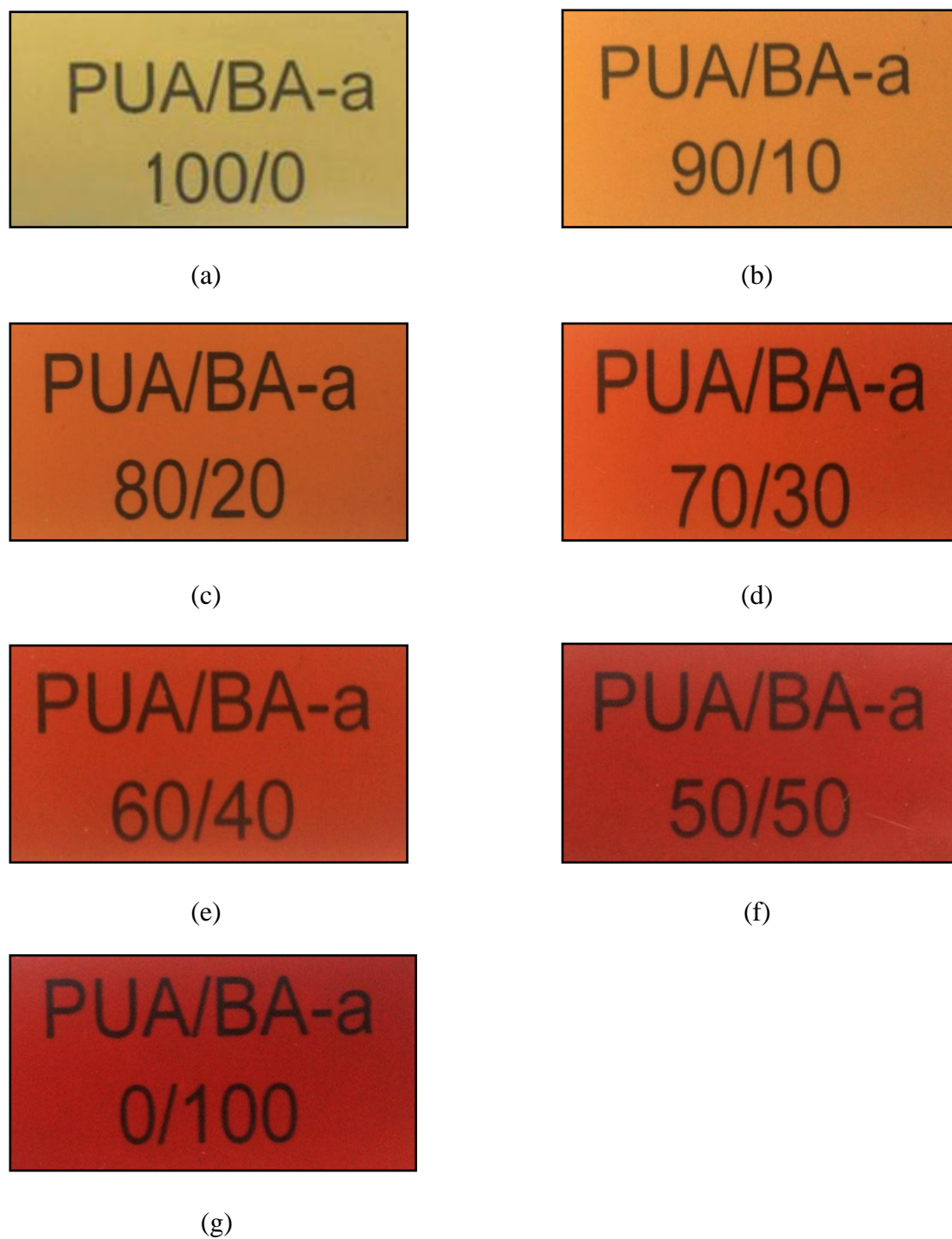


Figure 5.8 Photographs of PUA/BA-a alloy films at various composition: (a) 100/0, (b) 90/10, (c) 80/20, (d) 70/30, (e) 60/40, (f) 50/50, (g) 0/100.

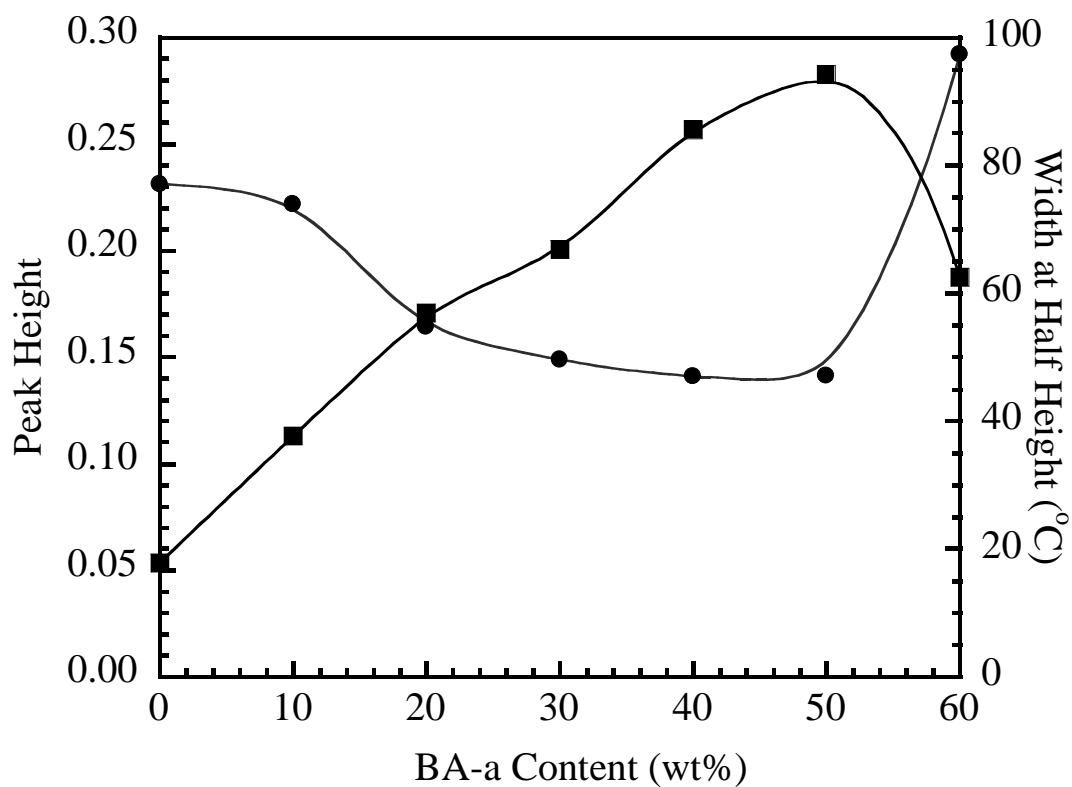


Figure 5.9 Height of $\tan \delta$ and width at half height of PUA/BA-a alloy films at various compositions: (●) Height of $\tan \delta$, (■) Width at half height of $\tan \delta$.

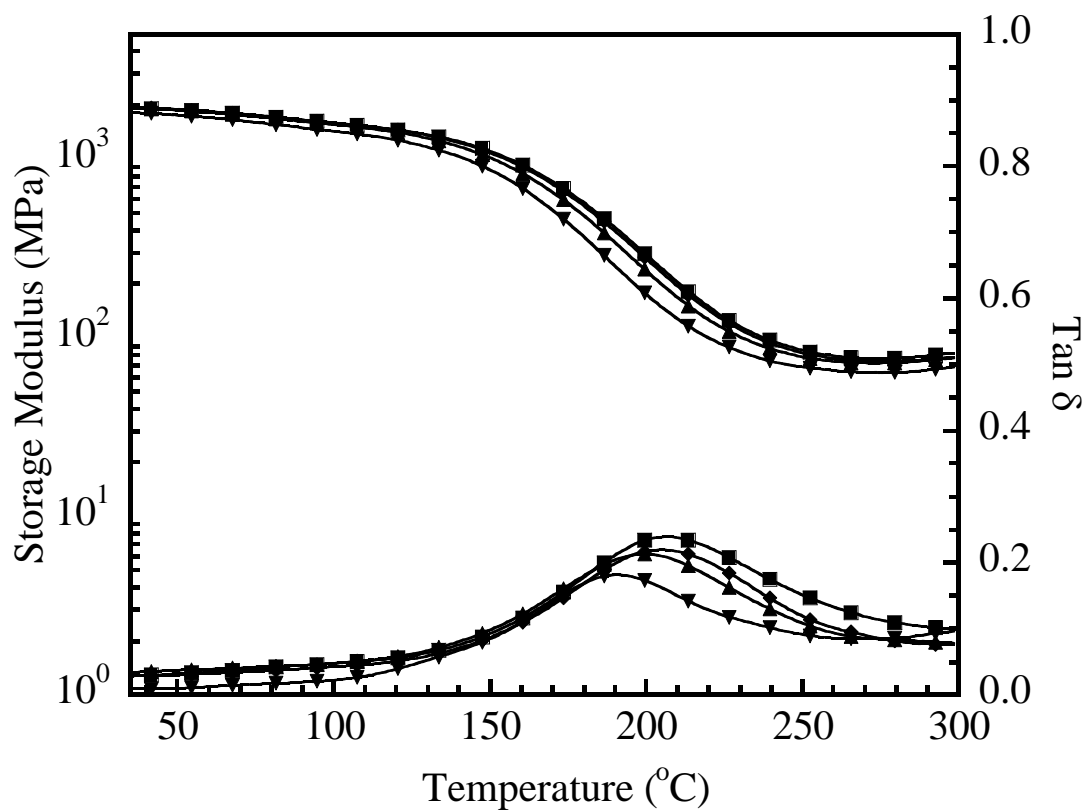


Figure 5.10 DMA curves of PUA/BA-a: 50/50 alloy films at various frequencies:

(▼) 1Hz, (▲) 10Hz, (◆) 25Hz, (■) 50Hz.

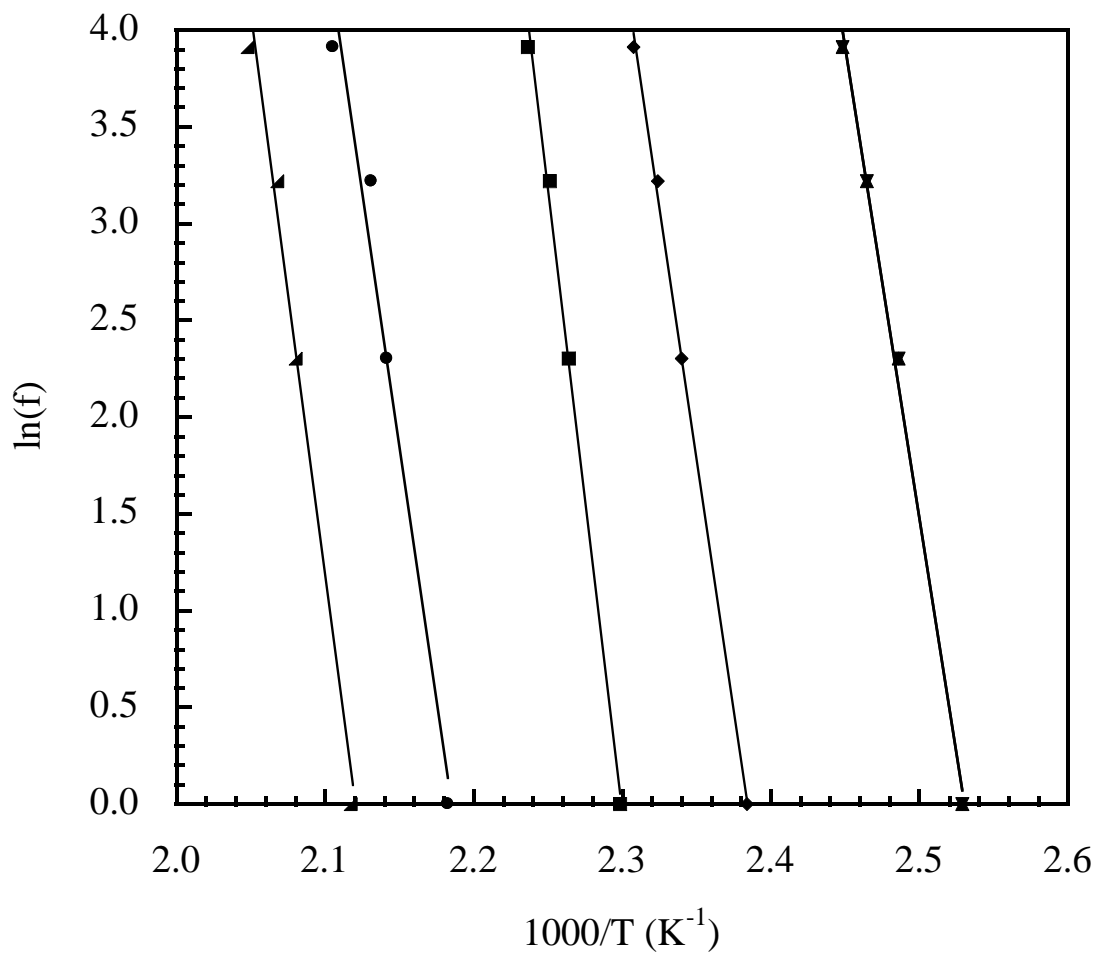


Figure 5.11 Arrhenius plot for the activation energy of the Tg of PUA/BA-a alloy films at various compositions: (▼) 100/0, (▲) 90/10, (◆) 80/20, (■) 70/30, (●) 60/40, (▲) 50/50.

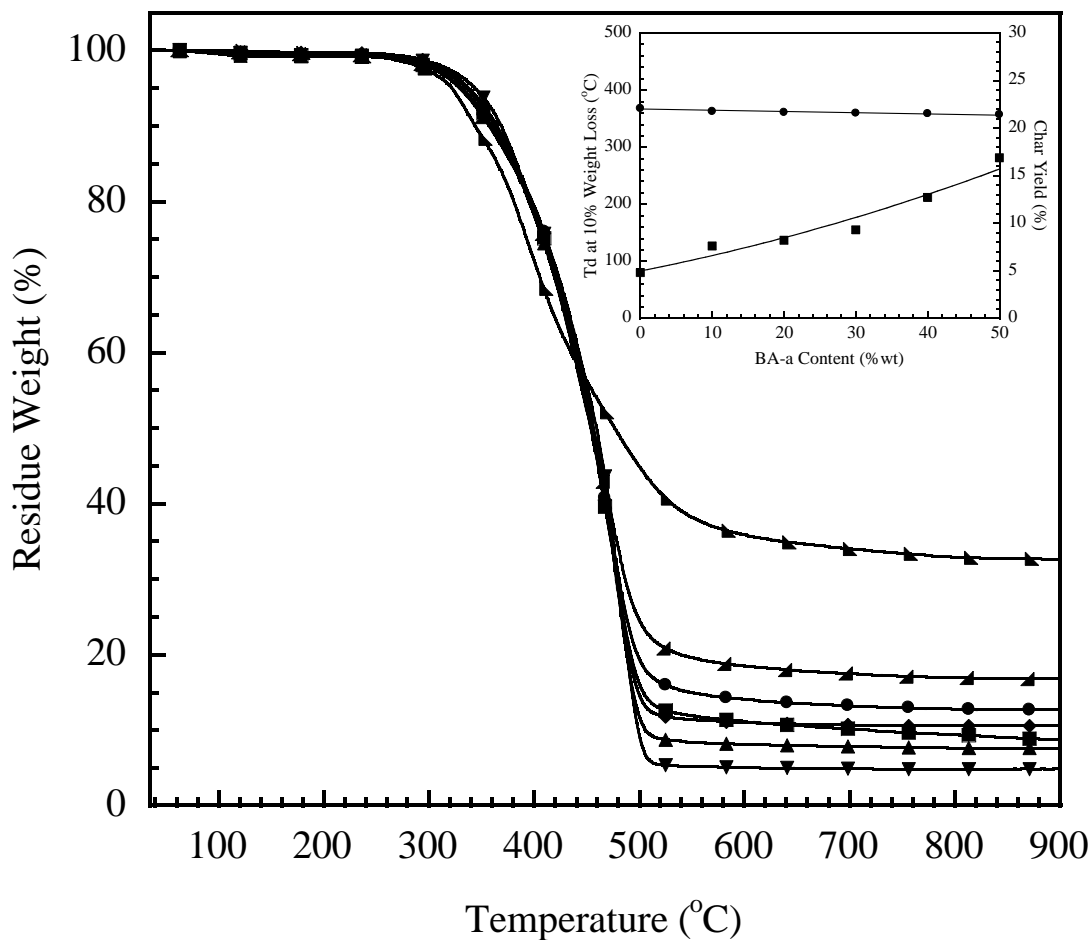


Figure 5.12 TGA thermogram of PUA/BA-a alloy films at various compositions:

(▼) 100/0, (▲) 90/10, (◆) 80/20, (■) 70/30, (●) 60/40, (◄) 50/50,
 (♣) 0/100.

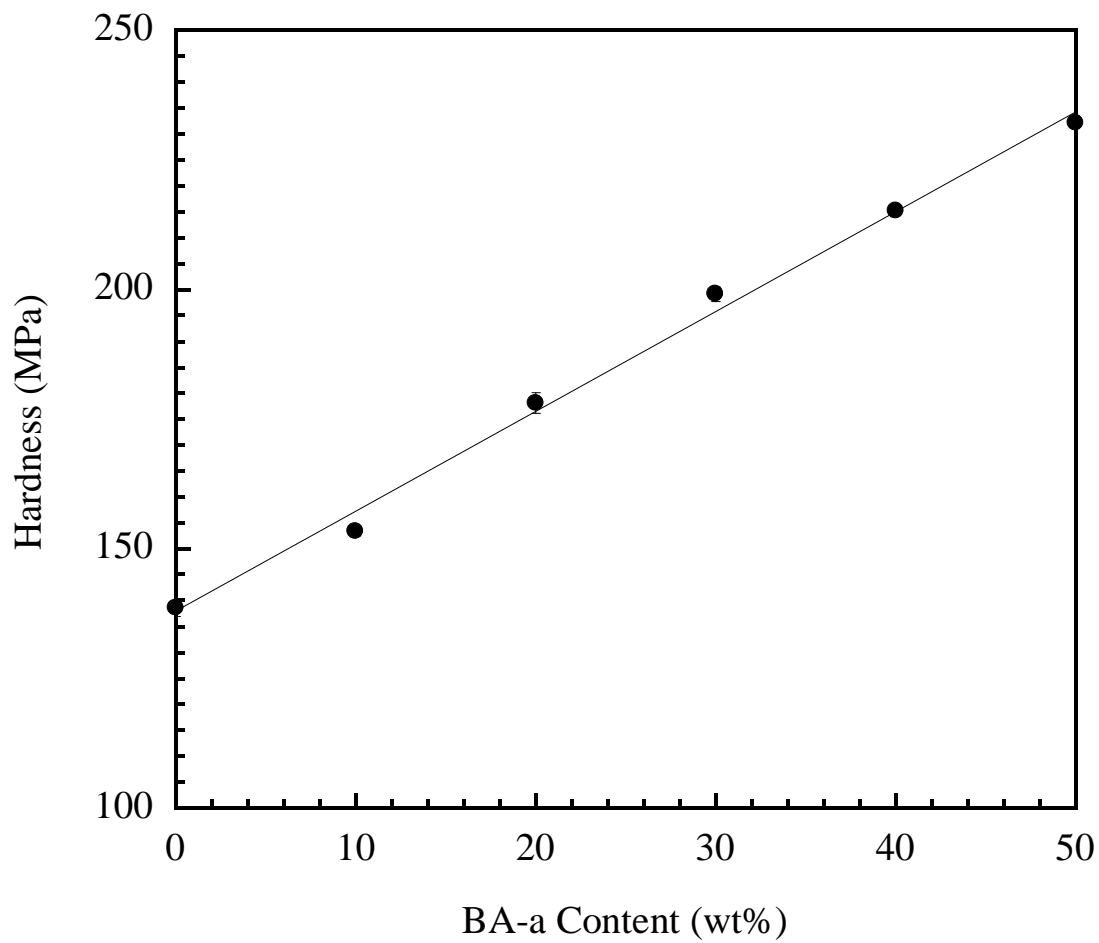


Figure 5.13 Hardness of PUA/BA-a alloy films at various compositions.

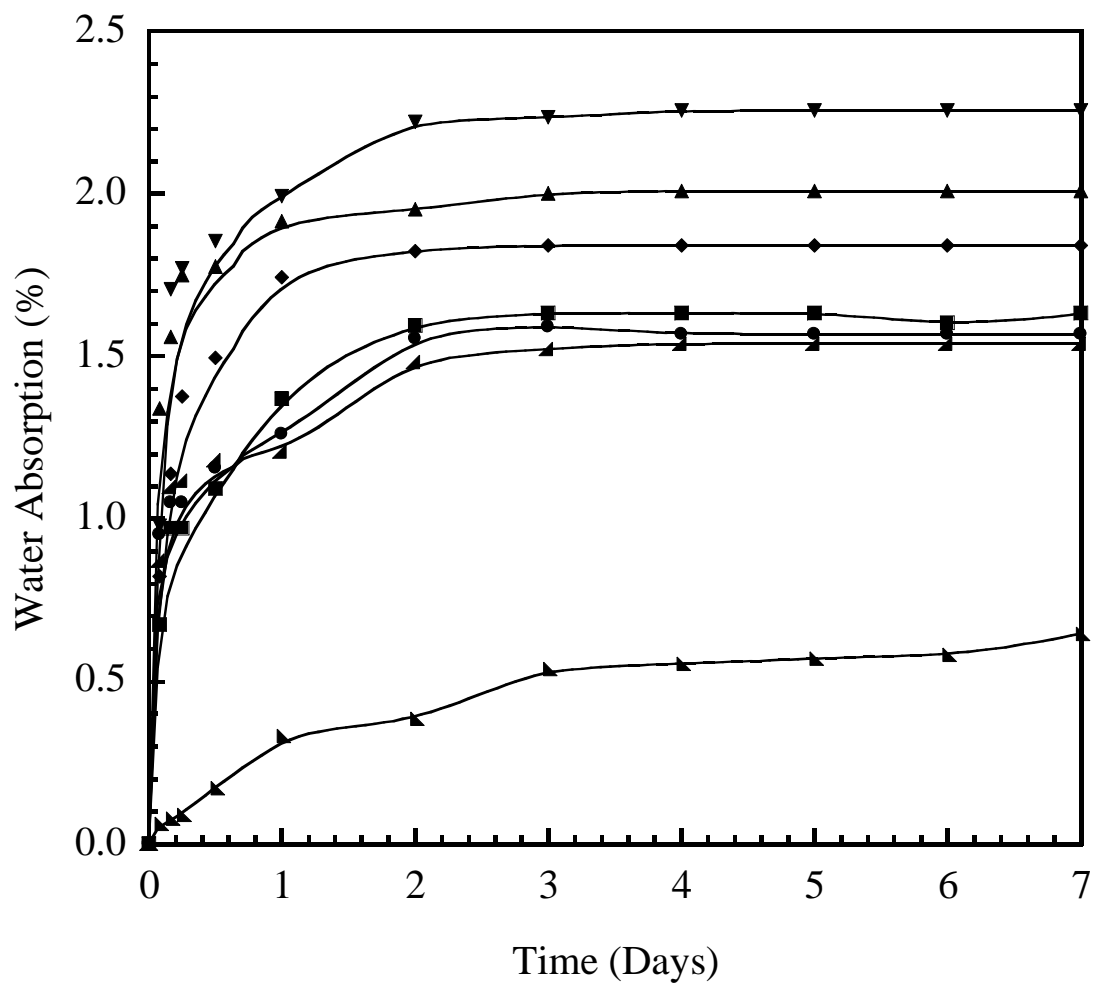


Figure 5.14 Water Absorption of PUA/BA-a alloy films at various compositions:

(▼) 100/0, (▲) 90/10, (◆) 80/20, (■) 70/30, (●) 60/40, (◄) 50/50,
 (►) 0/100.

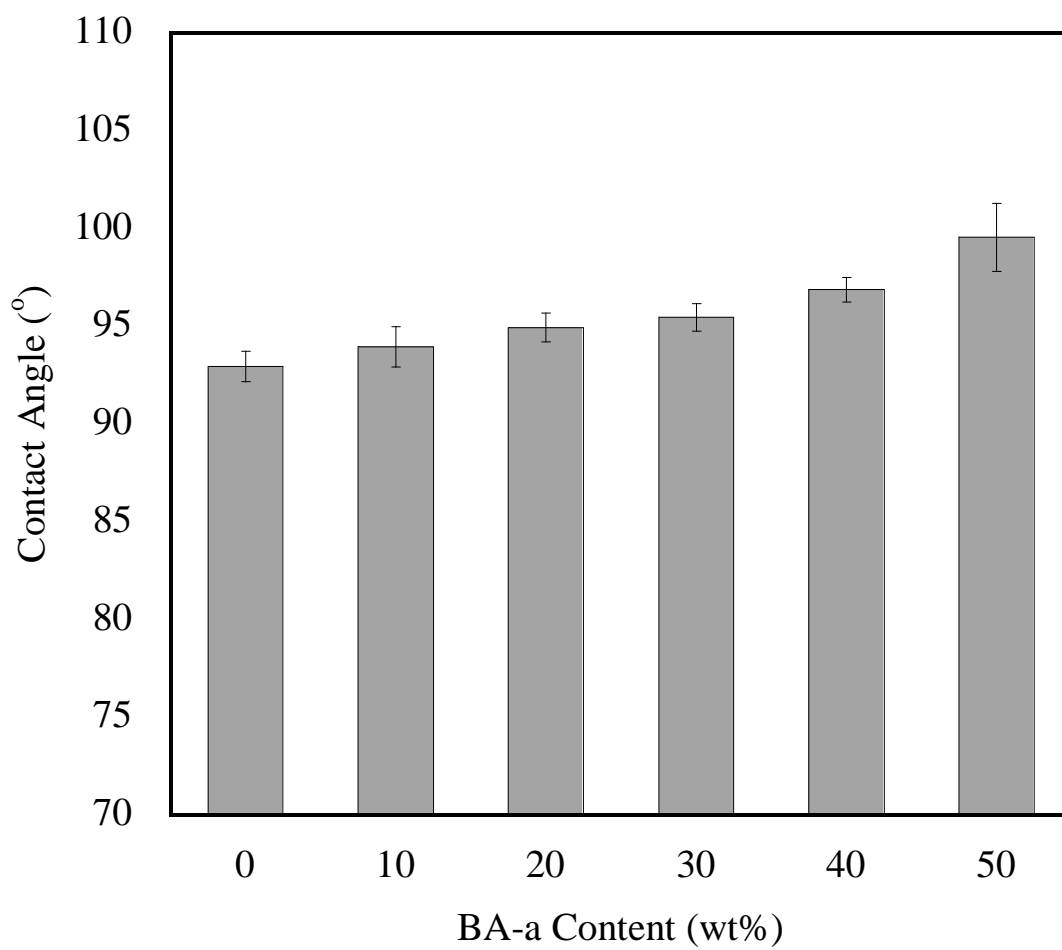


Figure 5.15 Contact angles of PUA/BA-a alloyfilms at various compositions.

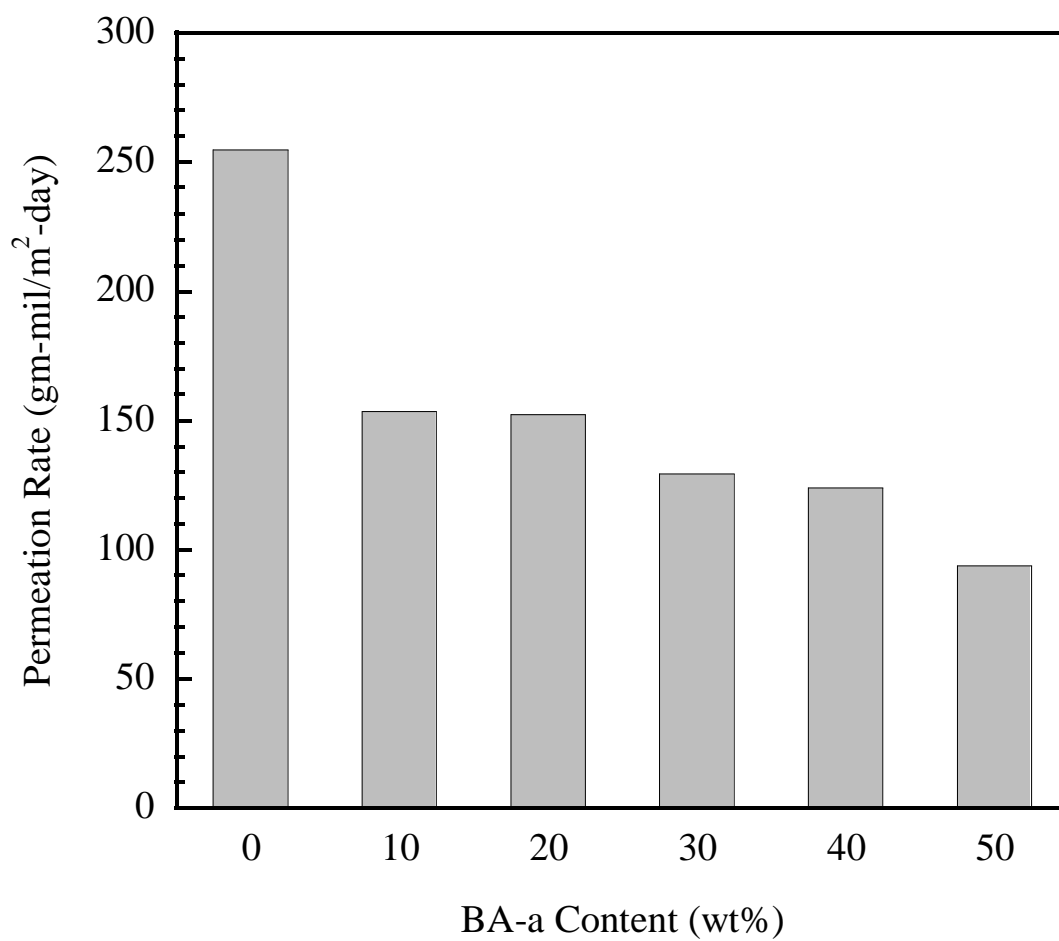


Figure 5.16 Permeation rates of PUA/BA-a alloy films at various compositions.

CHAPTER VI

CONCLUSIONS

Urethane acrylate-benzoxazine polymer network alloys based on different curing mechanisms of the two resins was developed. The obtained polymer alloys were processed by sequential cure method i.e. UV cure followed by thermal cure. The curing process significantly affected the network formation and the obtained properties of the alloys were systematically characterized.

From FT-IR results, the two major network forming reactions were observed. The UV curing produced the urethane acrylate network whereas benzoxazine network was found to form immediately by thermal curing step.

Thermal properties of the PUA/BA-a alloys were investigated by both DMA and TGA. The fully cured PUA/BA-a alloy films were transparent and showed only single glass transition temperature, suggesting high compatibility or no phase separation between the PUA and BA-a components. The storage modulus and glass transition temperature of the obtained polymer alloys increased with increasing the BA-a mass fraction in the hybrid polymer networks. Furthermore, Td at 10% weight loss of the resulting films exhibited relatively a high value whereas the char yield at 800°C substantially increased with an incorporation of the BA-a.

An incorporation the BA-a into PUA also resulted in higher surface hardness, and a desirable low water absorption value. The greater contact angle due to an addition of the BA-a suggested a potentially self-cleaning properties was also observed in the obtained polymer alloys.. Based on those properties evaluation, the PUA/BA-a polymer alloy film at 50/50 mass ratio exhibits the most promising characteristics to be utilized as a coating material.

The presence of BA-a in PUA network to form PUA/BA-a alloys was found to improve most properties of the UV curable PUA thus makes the alloy films suitable for e.g. coating application with high service temperature and enhanced mechanical integrity.

Based on the obtained results, the PUA/BA-a film has a potential use as high performance coating material such as for roof tile applications. Furthermore, properties of this film can also further be improved by some other modifications such as by adding filler e.g. TiO_2 for enhanced UV protection and self cleaning property.

REFERENCES

- [1] Jamshidi S., Yeganeh H. and Mehdipour-Ataei S.: Preparation and Properties of One-Pack Polybenzoxazine-Modified Polyurethanes with Improved Thermal Stability and Electrical Insulating Properties, **Polymer International**, 60, 126–135 (2011).
- [2] Chen L.J., Tai Q.L., Xing W.Y., Song L., Jie G.X. and Hu Y.: Thermal Properties and Flame Retardancy of an Ether-Type UV-Cured Polyurethane Coating, **Express Polymer Letters**, 4, 539-550 (2010).
- [3] Product information from CPAC Tile Roof Co., Ltd.
- [4] Chen C. and Chen M.: Synthesis, Thermal Properties, and Morphology of Blocked Polyurethane/Epoxy Full-Interpenetrating Polymer Network, **Journal of Applied Polymer Science**, 100, 323-328 (2006).
- [5] Pandit S.B. and Nadkarni V.M.: Sequential Interconnected Interpenetrating Polymer Networks of Polyurethane and Polystyrene: 1. Synthesis and Chemical Structure Elucidation, **Macromolecules**, 27, 4583-4594 (1994).
- [6] Yang J., Winnik M.A., Ylitalo D. and DeVoe R.J.: Polyurethane-Polyacrylate Interpenetrating Networks: 1. Preparation and Morphology, **Macromolecules**, 29, 7047-7054 (1996).
- [7] Takeichi T., Guo Y. and Agag T.: Synthesis and Characterization of Poly(urethane-benzoxazine) Films as Novel Type of Polyurethane/Phenolic Resin Composites, **Journal of Polymer Science Part A: Polymer Chemistry**, 38, 4165-4176 (2000).
- [8] Rimdusit S., Pirstpindvong S., Tanthapanichakoon W. and Damrongsakkul S.:

- Toughening of Polybenzoxazine by Alloying with Urethane Prepolymer and Flexible Epoxy: a Comparative Study, **Polymer Engineering & Science**, 45, 288-297(2005).
- [9] Yeganeh H., Razavi-Nouri M. and Ghaffari M.: Synthesis and Properties of Polybenzoxazine Modified Polyurethanes as A New Type of Electrical Insulators with Improved Thermal Stability, **Polymer Engineering & Science**, 48, 1329–1338(2008).
- [10] Baqar M., Agag T., Ishida H., and Qutubuddin S.: Poly(benzoxazine-co-urethane)s: A New Concept for Phenolic/Urethane Copolymers Via One-Pot Method, **Polymer**, 52, 307-317(2011).
- [11] Product information from Shikoku Chemical Operation [online]. Available from: <http://www.shikoku.co.jp/eng/product/labo/benzo/main.html> [2012, April 1].
- [12] Epsilon™ Products from Henkel Corporation [online]. Available from: <http://www.henkelepsilonresin.com/products.html> [2012, April 1].
- [13] Tsotra P., Weidmann U. and Christou P.: **Benzoxazine Chemistry: A New Material to meet Fire Retardant Challenges of Aerospace Interiors Applications**, Huntsman Advanced Material GmbH, CH-4057, Basel Switzerland.
- [14] Chattopadhyay D.K. and Webster D.C.: Thermal Stability and Flame Retardancy of Polyurethanes, **Progress in Polymer Science**, 34, 1068–1133 (2009)
- [15] Saunders K.J.: **Organic Polymer Chemistry**, 2nd Edition. New York: Chapman and Hall (1988).
- [16] Randall D., and Lee S.: **The Polyurethanes Handbook**, Huntsman

- International, United Kingdom: John Wiley and Sons (2002).
- [17] Sami A.S. and Anthony J.T.: Effect of Structure on the Thermal Stability of Photocurable Urethane Acrylate Formulations, **Journal of Polymer Sciences**, 43, 699-707 (2003).
- [18] Kim B.K. and Paik H.: UV-Curable Poly(Ethylene Glycol)-Based Polyurethane Acrylate Hydrogel, **Journal Polymer and Science Part A: Polymer Chemistry**, 37, 2703-2709 (1999).
- [19] Schauwecker H.H., Gerlach T., Planck H. and Bucherel E.S.: Isoelastic Polyurethane Prosthesis for Segmental Trachea Replacement in Beagle Dogs, **Artificial Organs**, 13, 216-218 (1989).
- [20] Pennings A.J., Knol K.E., Hoppen H.J., Leenslag J.W. and Lei B.V.D.: A Two-Ply Artificial Blood Vessel of Polyurethane and Poly(L-lactide), **Colloid and Polymer Science**, 268, 2-11 (1990).
- [21] Reghunadhan Nair C.P.: Advances in Addition-Cure Phenolic Resins, **Progress in Polymer Science**, 29, 422-423 (2004).
- [22] Takeichi T. and Agag T.: High Performance Polybenzoxazines as Novel Thermosets *High Performance*, **Polymers**, 18, 777-797 (2006).
- [23] Ishida H., U.S. Patent 5,543,516 (1996).
- [24] Ghosh N.N., Kiskan B. and Yagci Y.: Polybenzoxazines-New High Performance Thermosetting Resins: Synthesis and properties, **Progress in Polymer Science**, 32, 1344-1391 (2007).
- [25] Ning X. and Ishida H.: Phenolic Materials via Ring-Opening Polymerization

- of Benzoxazine: Effect of Molecular Structure on Mechanical and Dynamic Mechanical Properties, **Journal of Polymer Science Part B: Polymer Physics**, 32, 921-927 (1994).
- [26] Russell, V.M.; Koenig, J.L. Low, H.Y. and Ishida H.: Study of the Characterization and Curing of a Phenyl Benzoxazine Using N-15 Solid-State Nuclear Magnetic Resonance Spectroscopy, **Journal of Applied Polymer Science**, 70, 1413-1425 (1998).
- [27] Yagci Y., Kiskan B. and Ghosh N.N.: Recent Advancement on Polybenzoxazine-A Newly Developed High Performance Thermoset, **Journal of Polymer Science Part A: Polymer Chemistry**, 47, 5565-5576 (2009).
- [28] Henri U.: Raw Materials for Industrial Polymers, New York, Hanser Publishers (1988).
- [29] Fan J., Hu X. and Yue C.Y.: Static and Dynamic Mechanical Properties of Modified Bismaleimide and Cyanate Ester Interpenetrating Polymer Networks, **Journal of Applied Polymer Science**, 88, 2000-2006 (2003).
- [30] Klempner D., Sperling L.H. and Utracki L.A.: **Interpenetrating Polymer Networks**, Advances in *Chemistry Series*, 239, American Chemical Society, Washington DC (1994).
- [31] Reinhold S.: **UV Coatings: Basics, Recent Developments and New Applications**, Pigment & Resin Technology, 37, 6 (2007).
- [32] Come-back of EBC at the RadTech'05, **Coating**, Verlag Coating Thomas and Co, Switzerland, 12, 518-520 (2005).
- [33] Cui Y., Chen Y., Wang X., Tian. G. and Tang X.: Synthesis and

- Characterization of Polyurethane/Polybenzoxazine-Based Interpenetrating Polymer Networks (IPNs), **Polymer International**, 52,1246-1248 (2003).
- [34] Sun Y.Y. and Chen C.H.: Interpenetrating Polymer Network of Blocked Polyurethane and Phenolic Resin. I. Synthesis, Morphology, and Mechanical Properties, **Polymer Engineering and Science**, 51, 285-293 (2011).
- [35] Lin M.S. and Chiu G.A.: Curing Behavior and Mechanical Behavior of Fully and Semi-Interpenetrating Polymer Networks Based on Polyurethane and Acrylics, **Journal of Polymer Research**, 3, 165-171 (1996).
- [36] Lu C.H., Su Y.C., Wang C.F., Huang C.F., Sheen Y.C. and Chang F.C.: Thermal Properties and Surface Energy Characteristics of Interpenetrating Polyacrylate and Polybenzoxazine networks, **Polymer**, 49, 4852-4860 (2008).
- [37] **FT-IR Analyzer** from Polymer Center of Excellence [online]. Available from: <http://www.polymers-center.org/products/testinfo3.htm> [2012, April 1].
- [38] Thermogravimetric Analyzer from Mettler-Todleo International Inc. Available from: http://us.mt.com/us/en/home/phased_out_products/PhaseOut_An a/TGA_SDTA851e_Thermogravimetric_Analyzer.html [2012, April 1].
- [39] Micro-hardness Tester from TMC Measuring Instruments Pvt. Ltd. [online]. Available from: <http://www.ipfonline.com> [2012, April 1].
- [40] **Contact Angle Analyzer** from Astronics Technologies [online]. Available from: <http://www.astronics.sg/products.asp?lvl=1&catid=41> [2012, April 1].
- [41] Dunkers, J. and Ishida, H.: Reaction of Benzoxazine-based Phenolic Resins

- with Strong and Weak Carboxylic Acids and Phenols as Catalysts, **Journal of Polymer Science Part A: Polymer Chemistry**, 37, 1913-1921 (1999).
- [42] Rimdusit S., Bangsen W., and Kasemsiri P.: Chemorheology and Thermomechanical Characteristics of Benzoxazine-Urethane Copolymers, **Journal of Applied Polymer Science**, 120, 3669-3678 (2011).
- [43] Jubsilp C., Takeichi T., and Rimdusit S.: Property Enhancement of Polybenzoxazine Modified with Dianhydride, **Polymer Degradation and Stability**, 96, 1047-1053 (2011).
- [44] Rimdusit S., Mongkhonsi T., Kamonchaivanich P., Sujirote K. and Thiptipakorn S.: Effects of Polyol Molecular Weight on Properties of Benzoxazine-Urethane Polymer Alloys, **Polymer Engineering & Science**, 48, 2238-2246 (2008).
- [45] Nielsen L.E.: **Mechanical Properties of Polymers and Composites**, 1st ed, New York, Marcel Dekker (1974).
- [46] Nielsen L. E. and Landel R. F.: **Mechanical Properties of Polymers and Composites**, 2nd ed, New York: Marcel Dekker (1994).
- [47] Ishida H. and Allen D.J.: Physical and Mechanical Characterization of Near-zero Shrinkage Polybenzoxazines, **Journal of Applied Polymer Science**, 34, 1019-1030 (1996).
- [48] Vistap M.K. and Qiang W.: Multi-Frequency Dynamic Mechanical Thermal Analysis of Moisture Uptake in E-Glass/Vinylester Composites, **Composites Part B: Engineering**, 35, 299-304 (2004).
- [49] Kuzak S.G. and Shanmugam A.: Dynamic mechanical analysis of fiber

- reinforced phenolics, **Journal of Applied Polymer Science**, 73, 649–658 (1999).
- [50] Li G., Lee-Sullivan P. and Thring R.W.: Determination of Activation Energy for Glass Transition of An Epoxy Adhesive Using Dynamic Mechanical Analysis, **Journal of Thermal Analysis and Calorimetry**, 60, 377–390 (2000).
- [51] Martin J.S., Laza J.M., Morras M.L., Rodriguez M. and Leon L.M.: Study of The Curing Process of a Vinyl Ester Resin by Means of TSR and DMTA, **Polymer**, 41, 4203–4211 (2000).
- [52] Hill R., and Gilbert P.: High-Temperature Dynamic Mechanical Thermal Analysis of a Lithium Zinc Silicate Glass-Ceramic, **Journal of the America Ceramic Society**, 76, 417–425 (1993).
- [53] Barral L.: Determination of The Activation Energies for A and B Transitions of a System Containing a Diglycidyl Ether of Bisphenol A (DGEBA) and 1,3-Bisaminomethylcyclohexane (1,3-BAC), **Journal of Thermal Analysis and Calorimetry**, 41, 1463–1467 (1994).
- [54] Rimdusit S. and Ishida H.: Synergism and Multiple Mechanical Relaxations Observed in Ternary Systems Based on Benzoxazine, Epoxy and Phenolic Resins, **Journal of Polymer Science: Part B: Polymer Physics**, 38, 1687-1698 (2000).
- [55] Joseph P.V.; Mathew G.; Joseph K., Groeninckx G. and Thomas S. Dynamic Mechanical Properties of Short Sisal Fiber Reinforced Polypropylene composites, **Composites Part A: Applied Science and Manufacturing**, 34, 275-290 (2003).
- [56] Yu J., Yang J., Liu B. and Ma X.: Preparation and Characterization of

Glycerol Plasticized Pea Stacg/ZnO-Carboxymethylcellulose Sodium Nanocomposites, **Bioresource Technology**, 100, 2832-2841 (2009).

- [57] Bajpai S.K., Chand N. and Churasia V.: Investigation of Water Vapor Permeability and Antimicrobial Property of Zinc Oxide Nanoparticles-Loaded Chitosan-Based Edible Film, **Journal of Applied Polymer Science**, 115, 674-683 (2010).
- [58] Seo J., Jang W. and Han H.: Thermal, Optical, and Water Sorption Properties in Composite Films of Poly(ether imide) and Bismaleimides: Effect of Chemical Structure, **Journal of Applied Polymer Science**, 113, 777-783 (2009).
- [59] Hu Y., Topolkaev V., Hiltner A. and Bear E., Measurement of Water Vapor Transmission Rate in Highly Permeable Films, **Journal of Applied Polymer Science**, 81, 1624- 1633 (2001)
- [60] Simic S., Dunjic B., Tasic S., Bozic B., Jovanovic D. and Popovic I., Synthesis and Characterization of Interpenetrating Polymer Networks with Hyperbranched Polymer Through Thermal-UV Dual Curing, **Progress in Organic Coatings**, 63, 43-48 (2008).

APPENDICES

APPENDIX A

Dynamic Mechanical Properties of PUA/BA-a Alloy Films

Appendix A-1 Storage modulus of PUA/BA-a alloy films at various compositions at 35°C.

BA-a content (wt%)	Storage modulus (GPa)
0	1.3
10	1.6
20	2.0
30	2.1
40	2.1
50	2.3
60	2.3
100	2.6

Appendix A-2 Crosslink density of PUA/BA-a alloy films at various compositions.

BA-a content (wt%)	Storage modulus at rubbery plateau (T _g +50°C) (GPa)	Crosslink density (mol/m ³)
0	127.2	5554
10	101.6	5221
20	118.0	5443
30	116.9	5429
40	89.2	5027
50	83.5	4931

Appendix A-3 Glass transition temperature from DMA of PUA/BA-a alloy films at various compositions.

BA-a content (wt%)	Glass Transition Temperature (°C)
0	124
10	129
20	148
30	162
40	180
50	210
60	184
100	188

Appendix A-4 Activation Energy (ΔE_a) of the Tg of PUA/BA-a alloy films at various compositions.

BA-a content (wt.%)	Activation Energy (kJ/mol)
0	406
10	427
20	431
30	431
40	435
50	481

APPENDIX B

Thermal Properties of PUA/BA-a Alloy Films

Appendix B-1 Degradation temperature (Td) of PUA/BA-a alloy films at various compositions.

BA-a content (wt%)	Td at 10% weight loss
0	368
10	363
20	361
30	360
40	359
50	357
100	344

Appendix B-2 Char yield of PUA/BA-a alloy films at various compositions.

PU content (wt%)	Char yield at 800°C (%)
0	4.8
10	7.6
20	8.2
30	9.3
40	12.7
50	16.9
100	32.9

APPENDIX C

Mechanical Properties of PUA/BA-a Film Alloys

Appendix C-1 Surface hardness of PUA/BA-a alloy films at various compositions.

BA-a content (wt%)	Hardness (MPa)
0	139
10	154
20	178
30	199
40	215
50	232
100	404

APPENDIX D

Physical Properties of PUA/BA-a Alloy Films

Appendix D-1 Water absorption of PUA/BA-a alloy films at various compositions.

BA-a content (wt %)	Water Absorption (%) at 24 hrs.
0	1.99
10	1.92
20	1.79
30	1.37
40	1.26
50	1.21
100	0.33

Appendix D-2 Water contact angle of PUA/BA-a alloy films at various compositions.

BA-a content (wt%)	Water contact Angle (°)
0	92.9
10	93.9
20	94.9
30	95.5
40	96.9
50	99.6
100	107.7

Appendix D-3 Permeation rate of PUA/BA-a alloy films at various compositions.

BA-a content (wt%)	Permeation rate (gm-mil/m ² .day)
0	254
10	153
20	152
30	129
40	124
50	94
100	33

VITAE

Mr. Kasiphat Pudhom was born in Ayutthaya, Thailand, on July 19, 1984. He obtained a high school diploma in 2002 from Ayutthaya Witthayalai School. In 2006, he received a Bachelor's Degree in Chemical Engineering from the Department of Chemical Engineering, Faculty of Engineering, Suranaree University of Technology. After that, he pursued his graduate study for a Master Degree in Chemical Engineering at the Department of Chemical Engineering, Faculty of Engineering, Chulalongkorn University.